Reaction Rate Prediction via Group Additivity Part 1: H Abstraction from Alkanes by H and CH_3

R. Sumathi, H.-H. Carstensen,† and William H. Green, Jr.*

Department of Chemical Engineering, MIT, 77 Massachusetts Avenue, Cambridge, Massachusetts 02139

Received: February 22, 2001; In Final Form: May 2, 2001

Reliable estimates of high-pressure-limit reaction rates as a function of temperature are essential for the development of reaction sets that can be used to model complex chemical processes. As these reaction rates depend primarily on the thermodynamic properties of the reactants and the corresponding transition state, this work attempts to predict these properties within the framework of group additivity. Using ab initio calculations at the CBS-Q level, with additional HF/6-31G(d′) potential energy surfaces (PES) to define the hindrance potential for internal rotations, we calculate heats of formation ($\Delta_f H^{298}$), entropies (S^{298}), and heat capacity values ($C_p(T)$) of species involved in prototypical H abstraction reactions. From these, we derive new group additivity values (GAV) for transition-state-specific moieties. The new GAV allow rapid calculation of reaction rates for entire reaction families with good accuracy. This work presents a detailed description of the methodology and has its focus on H abstraction from alkanes by H and CH_3. Subsequent papers will apply this methodology to derive GAV for other reaction families of interest in combustion processes.

Introduction

An adequate description of complex chemical reaction systems found in industrial or environmental applications requires large compilations of reactions. The number of reactions in such mechanisms can easily reach up to 10 000, involving about 1000 different species. Development and maintenance of such big reaction sets is tedious, time-consuming, and prone to errors. Thus, kineticists consider more and more the use of computer-based tools which allow automated generation of reaction mechanisms.[1−13] Besides knowledge about all possible reaction types, such software needs to "know" the rates of individual reactions under the reaction conditions of the model. Experimental reaction rates are used if possible, but it is very difficult to derive reliable kinetic parameters over the entire range of reaction conditions even when good experimental data are available. The common procedure of extrapolating rate parameters to the conditions of interest can lead to severe errors. Alternative approaches are therefore needed.

High-pressure-limit rate constants can be calculated to a high level of accuracy using statistical mechanics and molecular parameters computed from an appropriate level of quantum chemistry. Statistical transition state theory is now well established experimentally,[14] and its connection to exact quantum scattering calculations is well understood.[15] Although a few cases have been found where the RRKM ergodicity assumption breaks down, TST rates are believed to be reliable for the vast majority of reactions of polyatomic molecules. Such reaction rates are not only of importance for high-pressure systems but also serve as input parameters to determine the pressure dependence of reactions in programs such as Chemdis[16] or MultiWell.[17] However, sophisticated ab initio calculations are limited to relatively small molecules due to CPU time and storage space restrictions. Reactions of practical interest frequently involve large reactants, and kinetic information for these can only be estimated from model systems. Estimation rules based on linear free energy relationship and other correlations have been known for a long time.[18−20] Although useful for certain specific applications, these rate rules have severe drawbacks and limitations such as thermodynamic inconsistency, missing information about Arrhenius factors (A factor) or lack of universality. Ranzi et al.[21] showed that rate estimation rules for abstraction reactions can be found based on a critical evaluation of literature data. Unfortunately, kinetic information for other reaction classes is too sparse to allow a similar approach.

As high-pressure-limit rate constants depict the kinetic behavior of systems in thermal equilibrium, one can calculate them from thermodynamic properties of the "species" involved. Benson[22] showed that thermodynamic properties of stable species as well as of radicals can be predicted on the basis of the assumption of group additivity. The appropriate group values (GAV) are derived from semiexperimental data. Bozzelli et al.[23] successfully demonstrated that first-principle calculations can also be used to deduce GAV's for some classes of molecules, for which experimental measurements are not possible. GAV for radicals are less comprehensively developed although O'Neal and Benson provide GAV for several alkyl and other free radical classes.[24] In 1992, Cohen[25] revised the group additivity difference method of O'Neal and Benson. The HBI method introduced by Bozzelli and co-workers[26] is essentially in line with Cohen's approach and provides improved prediction for thermodynamic properties of radicals. Bader and Bayles[27] recently provided the quantum mechanical basis for the classic concept of a functional group explaining why the group additivity approach works so well for both static and field-induced molecular properties.

In a series of papers, Cohen[28] applied the thermochemical kinetics formulation of conventional transition state theory to

* Corresponding author.
† Present address: Chemical Engineering Department, Colorado School of Mines, 329 Alderson Hall, Golden, CO 80401.

10.1021/jp010697q CCC: $20.00
Published on Web 06/22/2001

metathesis reactions of H and OH with a series of alkanes to extrapolate rate coefficients to temperature regimes outside the range of experiments. The magnitude of activation energy is determined generally in this model by adjusting the TST calculation to agree with the experimental k (298) values, while the entropy of activation is derived from the estimated structural and molecular properties of the activated complex. A central assumption of his simplified model is that all primary and, similarly, all secondary and all tertiary H atoms could be treated as equivalent. In other words, k_{total} is the sum of site-specific rate coefficients, $\Sigma_i n_{Hi} k_i$, where one sums either over primary, secondary, or tertiary hydrogen atoms. In a subsequent paper,[28d] Cohen examined the reliability of such an additive formulation for the abstraction rate coefficient in light of the dependency of barrier height on next-nearest neighbors and of the dependency of activation entropy on mass. He concluded that next nearest-neighbor effects are so small as to be indiscernible except where exceptionally good experimental data are available.

In this work, we try to extend the concept of group additivity to predict the thermochemical properties of transition states using quantum chemical calculations. The procedure is based on the idea that the reactive moiety remains nearly the same for all the reactions in a given class. Hence, the reactive moiety is expected to have a constant and transferable contribution toward the thermochemical properties of the transition state. Truong[29] used a similar assumption in his recent paper as a starting point for his reaction class transition state theory. However, his approach toward reaction rate prediction is different from ours in that he attempts to predict the thermal rate constant of any other reaction in the class from that of the principal reaction using two energetic properties, namely, the differential barrier height and the reaction energy.

The main objectives of this work are to (1) establish a methodology for the calculation of thermodynamic properties of transition states based on ab initio calculations, (2) extract GAV for "transition-state-specific" (reactive) moieties from these data, and (3) compare the computed reaction rates based on group additivity with literature data. In this paper, we present a set of GAV suitable for intermolecular hydrogen abstraction rate predictions from hydrocarbons by H, CH_3, and alkyl radicals. We further demonstrate that the rates predicted by group additivity are typically accurate within about a factor of 2 for all the reactions in a family.

The following reactions are considered for the present study:

$$R{-}H + H^* \rightarrow R^* + H_2$$

$$R{-}H + CH_3^* \rightarrow R^* + CH_4$$

$$H^* + H_2 \rightarrow H_2 + H^*$$

$$C_2H_5^* + C_2H_6 \rightarrow C_2H_6 + C_2H_5^*$$

$$C_2H_5^* + C_3H_8 \rightarrow C_2H_6 + i\text{-}C_3H_7^*$$

$$C_2H_5^* + i\text{-}C_4H_{10} \rightarrow C_2H_6 + t\text{-}C_4H_9^*$$

$$i\text{-}C_3H_7^* + C_3H_8 \rightarrow C_3H_8 + i\text{-}C_3H_7^*$$

$$i\text{-}C_3H_7^* + i\text{-}C_4H_{10} \rightarrow C_3H_8 + t\text{-}C_4H_9^*$$

$$t\text{-}C_4H_9^* + i\text{-}C_4H_{10} \rightarrow t\text{-}C_4H_{10} + t\text{-}C_4H_9^*$$

with R = CH_3, C_2H_5, C_3H_7 (1-, 2-), n-C_4H_9 (1-, 2-), i-C_4H_9 (1-, 2-), n-C_5H_{11} (1-, 2-, 3-), i-C_5H_{11} (1-, 2-, 3-, 4-), and q-C_5H_{11}. The numbers within parentheses indicate the position of the radical center. While the first two reaction sets describe the reactions of interest, we include the remaining ones to help us analyze the reactions in terms of the group additivity concept.

The remaining part of this paper is organized in the following way: First, we provide details of the calculations, including a description of the treatment of hindered rotors. Next, we compare calculated thermodynamic properties of stable molecules as well as of radicals with literature values and predictions from group additivity. Having shown the reliability of the calculations for reactants, we turn to the transition states. We calculate the thermodynamic properties of the reaction center, which could be called a "supergroup", as it contains several polyvalent atoms. Rate constants based on these supergroups are shown to compare well with "exact" transition state calculations of individual reactions. This supports the idea of basing rate predictions on transferable group values. We discuss possible ways to further subdivide the supergroups into groups in line with Benson's definition. Subsequently, we calculate reaction rates from GAV and compare them with literature data. This gives an idea of the achievable accuracy of this approach with the chosen methodology. We conclude with a discussion of the general value of this rate prediction method and outline future projects based on this concept.

Methodology

The high-pressure rate constant of a reaction A + B → products can be calculated based on transition state theory using the well-known formula

$$k(T) = L^{\ddagger}\kappa(T)V_m\frac{k_B T}{h}\exp(-\Delta H^{\ddagger}/(RT))\exp(\Delta S^{\ddagger}/R) \quad (1)$$

where $\Delta S^{\ddagger}$ and $\Delta H^{\ddagger}$ are, respectively, the entropy and enthalpy differences between the transition state geometry and the reactants, V_m is the molar volume at standard pressure (RT/P^o), and $L^{\ddagger}$ is the reaction path degeneracy. Finally, we include the tunneling correction factor, κ(T), to account for quantum mechanical tunneling contributions to reaction rates at low temperatures. ΔH(T) and $S(T)$ for the reactants can easily be calculated with the group additivity values H^{298}, S^{298}, and $C_p(T)$ given by Benson and co-workers.[22,30] To develop similar GAV for transition structures, we calculate H, S, and C_p for prototypical transition states from ab initio calculations via relations from statistical thermodynamics assuming ideal gas behavior.

Calculation of Thermochemical Properties. The total partition function, Q_{tot}, of any given molecule can be calculated within the framework of the rigid-rotor-harmonic-oscillator approximation

$$Q_{tot} = Q_{trans}Q_{rot}Q_{vib}Q_{elec} \quad (2)$$

$$Q_{trans} = V(2\pi M k_B T/h^2)^{3/2} \quad (3)$$

$$Q_{rot} = \frac{\sqrt{\pi}}{\sigma_{extern}}(8\pi^2 I_m k_B T/h^2)^{3/2} \qquad \text{with } I_m = I_x I_y I_z \quad (4)$$

$$Q_{vib} = \prod_i (1 - e^{-h\nu_i/(k_B T)})^{-1} \quad (5)$$

V is taken as the unit volume (1 cm^3), σ_{extern} is the external symmetry number of the molecule, and M is the molecular weight of the species. Molecular parameters needed for partition function calculations are the three moments of inertia (I_x, I_y, I_z) and the vibrational frequencies of the molecules. Q_{elec} is taken

as the spin degeneracy of the species (without spin contamination) for all species investigated in this work.

Torsional motions against low hindrances are treated as low-frequency vibrations in the harmonic oscillator model, thereby introducing errors in the calculated entropy, heat capacity, and heat of formation values. These motions are better treated as hindered internal rotations or, in the case of very small rotational barriers, as free rotations. The classical partition function of a one-dimensional free internal rotor is given by

$$Q_{\mathrm{fr}} = \frac{1}{\sigma_{\mathrm{ir}}} \frac{(8\pi^3 I_{\mathrm{ir}} k_{\mathrm{B}} T)^{1/2}}{h} \tag{6}$$

and it requires the knowledge of the reduced moment of inertia of the free rotor.

Hindered internal rotations are more difficult to deal with, as their energy levels depend on the magnitude and shape of the hindrance potential. The Schroedinger equation describing the restricted internal rotation can be written as

$$-\frac{h^2}{8\pi^2 I_{\mathrm{hir}}} \frac{\mathrm{d}^2}{\mathrm{d}\Phi^2}\psi_{\mathrm{hir}} + V\psi_{\mathrm{hir}} = E\psi_{\mathrm{hir}} \tag{7}$$

in which I_{hir} in the kinetic energy term denotes the reduced moment of inertia for the rotation under consideration. V is the rotational hindrance potential. Besides V, I_{hir} also depends on ϕ and is different for different conformers. Equation 7 is based on the assumption that one can separate internal rotations from each other and from the external rotation. It also assumes that the rotating group is rigid, i.e., that the potential energy terms coupling ϕ with other internal coordinates are negligible. However, one typically computes substantially different V_{hir} values if one holds the rotating group rigid versus if one allows all the degrees of freedom besides ϕ to relax. The former (rigid) method gives internal rotational barriers significantly higher than what one infers from experiment; herein we have chosen to allow the geometry to relax at each ϕ. The fact that the rotating group is not rigid means that I_{hir} is an effective moment of inertia and not the moment of inertia one would infer from the equilibrium geometry. In a series of papers,[31−33] Pitzer et al. showed that coupling of internal rotation with other internal rotors and with external rotation can be accounted for by choosing an appropriate reduced moment of inertia. We show in a separate paper[34] that it is not a bad approximation to use these reduced moments of inertia, $I^{(2,3)}$, as done in the present work. Finally, the separation of the internal rotor from other vibrational modes in eq 7 assumes that the vibrational frequencies are independent of ϕ. However, this is not really the case. As we show separately,[34] most of this ϕ dependence averages out while computing the hindered rotor partition function, Q_{hin}. However, if one computes Q using different conformers (e.g., trans, gauche) as the reference configuration, one finds that the computed Q's are somewhat different. In the present work, we Boltzmann-average the Q's computed using different conformers for stable molecules and radicals in cases where precise experimental data are available for comparison.

The most common way to compute Q_{hin} is to use the Pitzer−Gwinn tables for rigid internal rotors moving in a cosine potential. In literature, besides Pitzer−Gwinn tables, attempts have been made by researchers to provide an analytical form for Q_{hin} using various interpolation functions[35,36] and by approximating the Pitzer−Gwinn tables through polynomial fits.[37]

In the present work, partition functions for hindered rotations are calculated in a way very similar to that of Pitzer and Gwinn, but $V(\phi)$ was computed numerically instead of assuming a pure cosine potential. The reduced moments of inertia are calculated on the basis of Pitzer formulas,[31,32] which were recently reviewed by East et al.[38] Specifically, we use the $m = 2$, $n = 3$ approximation in terms of East et al. It means that the moments of the rotating groups are calculated with respect to an axis going through the center of mass of both rotating groups and the center of mass of the entire molecule. The reduced moment of inertia for rotation around this axis is approximated[39] as $1/I = 1/I_{\mathrm{L}} + 1/I_{\mathrm{R}}$, with I_{L} and I_{R} being the equilibrium geometry moments of the rotating groups. Instead of assuming or calculating rotational barriers, we determine the hindrance potential energy surface at the HF/6-31G(d′) level of calculation as a function of torsional angle and in stages of 10° or 20°. The potential energy surface thus obtained is then fitted to a Fourier series

$$\sum_m a_m \cos(m\varphi) + b_m \sin(m\varphi) \qquad \text{with } m \le 17$$

Subsequently, the rotational Schroedinger equation is solved numerically for the energy levels using the obtained Fourier coefficients in conjunction with cosine and sine basis functions. The partition function is evaluated by direct counting. This iterative procedure is continued with increased number of basis functions until Q_{hin} converges. The thermodynamic parameters H, S, and C_{p} are calculated from the ensemble energy averages, $\langle E\rangle^2$ and $\langle E^2\rangle$.

The molecular parameters needed to calculate the thermodynamic data are obtained from CBS-Q[40] calculations done with the Gaussian 98 program package.[41] HF/6-31G(d′) frequencies are scaled by 0.91844.[42] Moments of inertia are calculated from geometries optimized at the MP2/6-31G(d′) level. This geometry is also used as starting point for the calculation of rotational potentials which are done at HF/6-31G(d′) level. To calculate these potentials, we fix only the angle between both rotating groups and allow the remaining geometrical parameters to relax to a minimum. East et al.[38] investigated the dependency of the hindrance potential on the size of the basis set and the level of treatment. Although they recommend the use of large basis sets, we restrict ourselves to the HF/6-31G(d′) level, owing to the large number of molecules and internal rotations involved in this study.

Calculation of Heats of Formation of Stable Molecules and Radicals. The ab initio entropy and heat capacity values are direct results from the calculations, while the heat of formation data need to be obtained from the calculated absolute energy values. Instead of using the IUPAC definition of heat of formation, we calculate the heat of formation of molecules at 298.15 K on the basis of the calculated heat of atomization at 0 K (shown for methane)

$$\mathrm{CH_4} \rightarrow \mathrm{C_g} + 4\mathrm{H} \qquad \Delta H^{\mathrm{atomization}}$$

using the commonly adopted procedure in the literature.[43] $\Delta H^{\mathrm{atomization}}$ is calculated using ab initio results which are further corrected for spin−orbit interactions in C by −0.0875 kcal/mol[44]. To convert the atomization energies to heats of formations, we use the experimental heats of formation of C_g and H atoms at 0 K, 169.98 and 51.63 kcal/mol, respectively, and their corresponding enthalpy corrections $H^{298} - H^{\circ}$, 0.25 and 1.01 kcal/mol, respectively, from the JANAF tables.[45]

Petersson et al.[43] have shown that the accuracy of the CBS-Q energies is increased when applying bond additivity corrections

(BAC) for C−H and C−C bonds. To account for these known deficiencies, we correct our heat of formation data by adding their recommended corrections of −0.11 kcal/mol and −0.30 kcal/mol, respectively, for every C−H and C−C bond. The corrections described above serve only to compare our enthalpy results with experimentally based data, and they do not have an impact on the calculation of transition state properties described later (Tables 4−6).

We also calculated thermodynamic properties using group additivity with "Therm" software,[46] but we updated the GAV for the {C/C/H3}, {C/C2/H2}, {C/C3/H}, and {C/C4} groups with values given in ref 30. We used the hydrogen bond increment[26] method to calculate thermodynamic properties of radicals.

Derivation of Supergroup Values for Transition States. From the computed thermodynamic properties of the transition states, we can easily derive the contribution from the reactive moiety (supergroups) in terms of group additivity. We will use the reaction of propane with methyl radicals as an example to illustrate this:

$$CH_3CH_2CH_3 + CH_3^{\bullet} \leftrightarrows [CH_3{-}CH_2{-}H{-}CH_3] \leftrightarrows CH_3CH_2CH_2^{\bullet} + CH_4$$

The theoretically calculated heat of reaction ($\Delta_R H^{\ddagger}$) at 298 K for the formation of the transition state in the forward reaction is given by

$$\Delta_R H^{\ddagger}_{\text{forward}} = \Delta_f H(\text{ts}) - \Delta_f H(C_3H_8) - \Delta_f H(CH_3^{\bullet}) = E_0^{\text{forward}} + \Delta H^{0\rightarrow 298}(\text{ts}) - \Delta H^{0\rightarrow 298}(CH_3^{\bullet}) - \Delta H^{0\rightarrow 298}(C_3H_8)$$

$\Delta H^{0\rightarrow 298}$ denotes the thermal contribution to the enthalpy at 298.15 K. E_0^{forward} is the energy difference between the reactants, $CH_3 + C_3H_8$, and the transition state at 0 K. The same $\Delta_R H^{\ddagger}_{\text{forward}}$ value can also be obtained via group additivity

$$\Delta_R H^{\ddagger}_{\text{forward}} = \text{GA(ts)} - \text{GA}(C_3H_8) - \text{GA}(^{\bullet}CH_3) = H\{\text{C/C/H3}\} + H\{\text{C/C2/H2}\} + H\{\text{C/C/H2/−H/C/H3}\} - 2H\{\text{C/C/H3}\} - H\{\text{C/C2/H2}\} - H\{\text{CH3}\} = H\{\text{C/C/H2/−H/C/H3}\} - H\{\text{C/C/H3}\} - H\{\text{CH3}\}$$

The notations $H\{\text{C/C/H3}\}$ and $H\{\text{C/C2/H2}\}$ represent Benson's heat of formation group values for $-CH_3$ and $-CH_2-$ moieties, and H{CH3} represents the group equivalent heat of formation for CH_3 radicals. Finally, H{C/C/H2/−H/C/H3} symbolizes the enthalpy associated with the reaction center, $CH_2{-}H{-}CH_3$, which is not defined so far, and "−H" symbolizes the migrating H atom. Note that {C/C/H2/−H/C/H3} is not a group per se in the sense of Benson's definition because it contains three polyvalent atoms. Therefore, we will refer to it as a supergroup. Taking both expressions for $\Delta_R H^{\ddagger}_{\text{forward}}$ together, we obtain ΔH^{298} for this supergroup

$$\text{H\{C/C/H2/−H/C/H3\}} = \Delta_R H^{\ddagger}_{\text{forward}}\,(\text{ab initio}) + \text{H\{C/C/H3\}} + \text{H\{CH3\}}$$

As in the case of the bond dissociation energies, we only need the difference between calculated transition state and reactant heat of formations (or energies) for the calculation of the heat of formation value of the supergroup. With the assumption that some uncertainties in the ab initio values are systematic (as in isodesmic reactions), we expect that the difference will be more accurate. To further improve the accuracy or to check for consistency, we can repeat the same calculation for the reverse reaction and obtain for the same supergroup a second value, this time based on different ab initio and GA values

$$\Delta_R H^{\ddagger}_{\text{reverse}} = E_0^{\text{reverse}} + \Delta H^{0\rightarrow 298}(\text{ts}) - \Delta H^{0\rightarrow 298}(CH_4) - \Delta H^{0\rightarrow 298}(C_3H_7^{\bullet})$$

and

$$\Delta_R H^{\ddagger}_{\text{reverse}} = \text{GA(ts)} - \text{GA}(n\text{-}C_3H_7^{\bullet}) - \text{GA}(CH_4) = H\{\text{C/C/H3}\} + H\{\text{C/C2/H2}\} + H\{\text{C/C/H2/−H/C/H3}\} - H\{C_3H_7\}^{\text{HBI}} - H\{CH_4\}$$

leading to

$$H\{\text{C/C/H2/−H/C/H3}\} = \Delta_R H^{\ddagger}_{\text{reverse}}(\text{ab initio}) - H\{\text{C/C/H3}\} - H\{\text{C/C2/H2}\} + H\{n\text{-}C_3H_7\}^{\text{HBI}} + H\{CH_4\}$$

The superscript HBI indicates that the hydrogen bond increment method[26] is used to determine the thermodynamic properties of the radical C_3H_7, and H{CH4} denotes the GAV for CH_4. Analogous formulas allow one to determine the intrinsic entropy (S_{int}^{298}) and the temperature-dependent C_p^T group additivity values for transition state supergroups. However, in the case of the intrinsic entropy, corrections for the symmetry (σ) of the reactants and transition state have to be taken into account so that for the forward reaction of our example the following symmetry-correction term

$$S_{\text{int}}\{\text{C/C/H2/−H/C/H3}\} = \Delta_R S^{\ddagger}_{\text{forward}} + S\{\text{C/C/H3}\} + S\{\text{CH3}\} - R\ln(\sigma_{CH_3}{}^{*}\sigma_{C_3H_8}/\sigma_{\text{ts}})$$

is obtained.

Calculation of the Tunneling Correction Factor, $\kappa(T)$. The rate calculated using the supergroup values does not include the tunneling contributions at low temperatures. To account for quantum mechanical tunneling effects, we calculate, the transmission coefficient κ(T) using the simple Wigner perturbation theory formula[47]

$$\kappa(T) = 1 + \frac{1}{24}\left(1.44\frac{\nu_i}{T}\right)^2$$

wherein ν_i is the magnitude of the imaginary frequency in cm^{-1} corresponding to the one-dimensional reaction coordinate at the transition state and T is the temperature in Kelvin.

Results and Discussion

The main problem with the attempt to characterize thermodynamic properties of transition states via ab initio calculations is that one has no direct means to prove the accuracy of the results. Thus, one is left with indirect justifications such as comparison of results for stable species or verification of theoretically computed reaction rates based on transition state properties with experimental data. Consequently, we first draw our attention toward the stable species and radicals before dealing with transition state structures.

Thermodynamics of Stable Species. Our results for the thermodynamic properties of H_2 and C_1-C_5 alkanes are given in Table 1 together with GA-based predictions and data from literature. From the many available thermochemical databases

TABLE 1: Comparison of Calculated Thermodynamic Properties of H_2 and C_1-C_5 Alkanes with Group Additivity Predictions (GA[22,26]) and Experimental Data (NIST = NIST Webook[48A] or NIST Standard Reference Database 25[48b])[a]

species	method/source	$\Delta_f H^{298}$	S^{298}	C_p^{300}	C_p^{400}	C_p^{500}	C_p^{600}	C_p^{800}	C_p^{1000}	C_p^{1500}	C_p^{inf}
	ab initio	−1.11	31.06	6.96	6.96	6.96	6.96	7.01	7.12	7.63	7.91
H2	GA	0.00	31.20	6.90	−	7.00	−	7.10	7.20	7.70	
	NIST	0.00	31.23	6.90	6.98	6.99	7.01	7.08	7.22	7.72	
	ab initio	−17.89	44.44	8.46	9.54	10.90	12.30	14.89	17.04	20.62	25.83
CH4	GA	−17.90	44.50	8.50	−	11.10	−	15.00	17.20	20.70	
	NIST	−17.90	44.51	8.54	9.68	11.08	12.48	15.04	17.16	20.66	
	ab initio	−19.98	54.71	12.53	15.50	18.43	21.11	25.61	29.13	34.78	42.72
C2H6	GA	−20.00	54.86	12.46	15.84	18.88	21.58	26.08	29.66	35.22	
	NIST	−20.04	54.88	12.60	15.65	18.63	21.32	25.80	29.29	34.87	
	ab initio	−24.84	64.55	17.61	22.29	26.67	30.61	36.76	41.54	49.09	59.61
C3H8	GA	−25.00	64.26	17.96	22.81	27.12	30.92	37.16	41.90	49.47	
	NIST	−25.02	64.53	17.67	22.47	26.91	30.76	36.99	41.73	49.21	
	ab initio	−29.96	73.41	23.84	29.68	35.19	40.05	47.95	53.97	63.43	76.50
n-C4H10	GA	−30.00	73.66	23.46	29.78	36.36	40.26	48.24	54.24	63.72	
	NIST	−30.38	74.09	23.65	29.82	35.53	40.46	48.37	54.34	63.67	
	ab initio	−35.62	81.71	30.21	37.19	43.80	49.65	59.17	66.43	77.78	93.39
n-C5H12	GA	−35.00	83.06	28.96	36.76	43.60	49.60	59.32	66.58	77.97	
	NIST	−35.09	83.13	28.83	36.46	43.64	49.90	59.90	67.30	79.00	
	ab initio	−32.02	70.43	23.24	29.64	35.47	40.46	48.38	54.33	63.62	76.50
i-C4H10	GA	−32.40	69.87	23.27	29.78	36.51	40.48	48.50	54.44	64.10	
	NIST	−32.07	70.41	23.22	29.74	35.67	40.72	48.67	54.60	63.82	
	ab initio	−36.70	82.14	28.67	36.34	43.38	49.47	59.19	66.48	77.82	93.39
i-C5H12	GA	−36.60	81.45	28.77	36.75	43.75	49.82	59.58	66.78	78.35	
	NIST	−36.74	82.10	28.56	36.54	43.80	50.20	60.50	68.40	81.00	
	ab initio	−40.87	73.72	29.23	37.27	44.49	50.60	60.16	67.24	78.22	93.39
q-C5H12	GA	−39.90	72.53	29.33	37.75	45.05	51.28	61.01	67.87	78.54	
	NIST*	−40.14	73.21	29.05	37.28	44.69	51.30	62.40	71.20	86.00	

[a] $\Delta_f H^{298}$ is given in kcal/mol, and S^{298} and C_p^T data are in cal mol^{-1} K^{-1}. The calculated properties are given for the most stable conformer. See text for discussion of conformer contributions to bulk properties. The *q*-C5H12 C_p values given in the NIST webbook differ significantly from those in Stull, D. R.; Westrum, E. F., Jr.; Sinke, G. C. *The Chemical Thermodynamics of Organic Compounds*; Wiley: New York, 1969. C_p^{300} = 29.21; C_p^{400} = 37.55, C_p^{500} = 45.00; C_p^{600} = 51.21; C_p^{800} = 60.78; C_p^{1000} = 67.80; C_p^{1500} = N/A.

we herein restrict ourselves to the Web-based NIST database[48a] wherever possible and use data from the NIST "Structure and Properties" database[48b] otherwise.

A glance at the $\Delta_f H^{298}$ results in Table 1 reveals that our calculated data are in excellent agreement with the reference data. The nonzero heat of formation for H_2 results from the use of atomization energies for its calculation in combination with the fact that CBS-Q calculations over-predict the H−H bond strength. The good agreement for the hydrocarbons is expected because we used Petersson's BAC. The more accurate treatment of low frequency vibrations as hindered rotations instead of harmonic oscillations has only a minor impact on the enthalpy at low temperatures. Consequently, our results are essentially equal to those presented by Petersson et al. [43].

We observe nearly as good agreement with entropy values, with excellent agreement for H_2, CH_4, C_2H_6, C_3H_8, and *t*-C_4H_{10}. The deviations for these species are generally less than 0.2 cal/(mol K) when compared with the NIST data. Entropy values for *n*-C_4H_{10}, *n*-C_5H_{12} deviate significantly more from experimental values (0.6 and 1.4 cal/(mol K), respectively) and GA predictions. The explanation lies in contributions from different conformers to the bulk entropy. Our chosen approximation for the hindered rotations does not take proper coupling between internal rotation and external rotation into account. With either an improved coupling, I[(3,4)], or through approximating the bulk entropy to the Boltzmann averaged contributions from the conformers, we obtain entropy values of 74.18 and 73.99 cal/(mol K), respectively, for *n*-butane. These values are in excellent agreement with the literature value. Recent ab initio based entropy calculations of Chen et al.[49] Gang et al.[50] and DeTar [51] yield S^{298} values in the range of 74.0−74.1 cal/(mol K) showing that our results are very reasonable.

The predicted C_p values in Table 1 are generally in excellent agreement, within a few tenth of a cal/(mol K), with experimental values. As seen in the case of $\Delta_f H^{298}$ and S^{298} values, an improved agreement in C_p values is obtained for larger alkanes after Boltzmann-averaging the conformational contributions. It is appropriate to mention that the NIST tabulated C_p values for isopentane and *q*-pentane seem wrong at high temperatures. Given the uncertainties in the reference data it appears that our calculated data are very reliable. DeTar[51] reports larger discrepancies at higher temperatures (1000K) between his calculated C_p data and literature. The main reason for this is that DeTar considers all internal motions as vibrational modes, which will over-predict the heat capacity at high temperatures. Our hindered rotor treatment prevents this.

In summary, we are able to reproduce thermodynamic data of primary, secondary and tertiary alkanes very well. This gives us confidence that the chosen methodology is adequate for stable molecules. To approach our goal − the characterization of thermodynamic properties of transition states − we now take a closer look at the results for the radicals.

Thermodynamics of Radicals. In Table 2 we compare our ab initio results for radicals with GA and literature data. Again, we restrict ourselves to experimental values published by NIST.[48a,b] As mentioned above, the raw data were corrected for small systematic errors in C−H and C−C bonds.[43] With respect to heat of formation energies, Table 2 shows that CBS-Q calculations over-predict these relative to experimental data (NIST) by not more than ∼2 kcal/mol (except for tertiary radicals), which is well within the limits of experimental uncertainties. In general, agreement between ab initio results and GA data is even better than between calculated and NIST values with the only exception being the 2-methyl-prop-1-yl radical.

In the case of the CH_3 radical, we observed problems in calculating the low-frequency umbrella mode vibration. The calculated value of 289 cm^{-1} is more than a factor of 2 lower

TABLE 2: Comparison of Calculated and Literature Data on Thermodynamic Properties of H and C_1-C_5 Alkyl Radicals[a]

radical	method/source	$\Delta_f H^{298}$	S^{298}	C_p^{300}	C_p^{400}	C_p^{500}	C_p^{600}	C_p^{800}	C_p^{1000}	C_p^{1500}	C_p^{inf}
	ab initio	52.10	27.39	4.97	4.97	4.97	4.97	4.97	4.97	4.97	4.97
H	GA	52.10	27.40	5.00	5.00	5.00	5.00	5.00	5.00	5.00	
	NIST	52.10	27.42	4.97	4.97	4.97	4.97	4.97	4.97	4.97	
	ab initio	35.41	46.40	9.30	10.06	10.81	11.53	12.88	14.09	16.30	19.87
CH3	GA	35.10	46.40	8.80	–	10.60	–	13.20	14.50	16.80	
	NIST	34.82	46.41	9.26	10.05	10.81	11.54	12.89	14.09	16.28	
	ab initio	29.58	59.37	12.40	14.83	17.19	19.31	22.88	25.68	30.23	
C2H5	HBI	29.00	59.65	11.81	14.63	17.13	19.34	23.06	25.93	30.60	36.76
	NIST	28.44	–	11.62	14.39	17.45	19.65	23.28	25.88	30.33	
	ab initio	25.05	69.35	17.40	21.53	25.32	28.60	33.92	38.00	44.49	53.65
n-C3H7	HBI	24.00	69.05	17.19	21.45	25.21	28.52	34.00	38.15	44.79	
	NIST	23.90	68.50	17.11	21.34	25.69	28.99	34.35	38.22	44.60	
	ab initio	19.85	78.35	23.12	28.65	33.72	38.10	45.13	50.46	58.85	70.54
n-C4H9	HBI	19.00	78.45	22.69	28.42	33.45	37.86	45.08	50.48	59.04	
	NIST	18.00	–	22.60	28.30	33.90	38.30	45.40	50.60	58.80	
	ab initio	14.53	87.09	29.23	35.96	42.20	47.61	56.31	62.88	73.17	87.43
n-C5H11	HBI	14.00	87.85	28.19	35.39	41.69	47.20	56.16	62.81	73.29	
	NIST	13.00	–	28.10	35.20	42.20	47.70	56.50	62.90	73.00	
	ab initio	18.67	76.43	23.05	28.83	33.99	38.38	45.35	50.61	58.90	70.54
i-C4H9 (1°)	HBI	16.60	75.77	22.73	28.52	33.59	38.02	45.23	50.60	59.41	
	NIST	17.00	75.20	22.30	28.20	34.00	38.50	45.60	50.70	59.10	
	ab initio	13.32	85.72	28.43	35.56	41.99	47.50	56.27	62.86	73.16	87.43
i-C5H11 (1°,1)	HBI	12.00	85.17	28.23	35.49	41.83	47.36	56.31	62.93	73.66	
	NIST	–	–	–	–	–	–	–	–	–	
	ab initio	12.76	85.54	28.79	35.94	42.40	47.91	56.61	63.12	73.30	87.43
i-C5H11 (1°,4)	HBI	12.00	84.87	28.00	35.39	41.84	47.42	56.42	63.03	73.66	
	NIST	–	–	–	–	–	–	–	–	–	
q−C5H11	ab initio	10.36	80.19	28.96	36.42	43.00	48.53	57.15	63.55	73.52	87.43
	HBI	9.10	79.12	28.74	36.43	43.00	48.63	57.51	63.81	73.63	
	NIST	8.00	–	28.40	36.20	43.60	49.30	58.10	64.20	73.60	
i-C3H7	ab initio	22.24	68.75	16.42	20.21	23.98	27.39	33.04	37.37	44.20	53.65
	HBI	21.35	68.77	16.66	20.45	24.10	27.48	33.18	37.53	44.46	
	NIST	22.00	66.70	16.80	20.90	25.10	28.40	33.80	37.90	44.60	
	ab initio	17.44	79.30	22.07	27.29	32.35	36.84	44.16	49.74	58.48	70.54
n-C4H9 (2°)	HBI	16.35	78.79	21.92	27.01	31.87	36.86	43.89	49.58	58.56	
	NIST	16.00	–	22.30	27.80	33.30	37.70	44.80	50.20	58.90	
	ab initio	11.61	87.79	27.79	34.44	40.79	46.37	55.40	62.23	72.86	87.43
n-C5H11 (2°,2)	HBI	11.35	89.56	27.42	33.98	40.11	45.70	54.97	61.91	72.81	
	NIST	12.00	–	27.80	34.80	41.60	47.10	55.90	62.60	73.10	
	ab initio	12.33	86.83	27.92	34.57	40.87	46.41	55.37	62.16	72.79	87.43
n-C5H11 (2°,3)	HBI	11.35	87.96	27.25	33.61	39.68	45.27	54.61	61.63	72.66	
	NIST	–	–	–	–	–	–	–	–	–	
	HBI	10.59	86.23	28.22	34.94	41.25	46.75	55.64	62.36	72.88	87.43
i-C5H11 (2°,3)	HBI	8.95	86.58	27.23	33.98	40.26	45.92	55.23	62.13	73.18	
	NIST	–	–	–	–	–	–	–	–	–	
	ab initio	13.74	74.84	21.70	26.60	31.55	36.06	43.55	49.29	58.26	70.54
tert-Butyl	HBI	12.00	73.73	22.49	27.30	31.96	36.33	43.75	49.42	58.68	
	NIST	11.00	72.10	22.60	28.40	33.60	38.10	45.30	50.70	59.30	
	ab initio	9.51	86.28	27.13	33.35	39.57	45.18	54.42	61.45	72.42	87.43
i-C5H11 (3°,2)	HBI	7.00	85.31	27.99	34.27	40.20	45.67	54.83	61.75	72.93	
	NIST	6.70	–	28.10	35.40	41.90	47.50	56.40	63.00	73.50	

[a] Calculations were performed for the most stable conformer. $\Delta_f H^{298}$ is given in kcal/mol, and S^{298} and C_p^T data are in cal mol^{-1} K^{-1}. "HBI" indicates group additivity based predictions using the hydrogen bond increment method,[26] with respect to "NIST", see the caption of Table 1. The numbers in parentheses of the first column signify the nature and position of the radical center.

than the experimental value of 606 cm^{-1} [52,53]. This error leads to wrong entropy and low-temperature C_p values and it introduces a small error on the thermal correction of the enthalpy. As CH_3 is a reactant in one entire set of H abstraction reactions we are interested in, we decided to calculate the thermodynamic properties of methyl radicals by using the experimental frequency in order to avoid systematic errors. A closer look at the optimized geometries of other alkyl radicals reveals that their radical center are nonplanar unlike in the methyl case. Furthermore, in these radicals the lowest frequency vibration corresponds to out-of-plane methylene bend. The calculated harmonic frequency for this mode in radicals is in reasonable agreement with experiment. Therefore, we conclude that the problem observed in the case of the CH_3 frequency is unique.

The relative errors between radicals and their parent alkanes can best be seen by calculating the bond dissociation energies (BDE) at 0 and 298 K. Table 3a compares our results with GA predicted BDE's. In addition, the fourth column in Table 3 shows the differences between calculated BDE's at 0 and 298 K which is a measure of the change of thermal energy in dissociation reaction. The differences in BDE's between group additivity prediction and ab initio calculation are in general small and positive because the heats of formations of the alkanes were found to be closer to the GA data than those of the radicals. We further see that the deviation for the bond dissociation of H_2 is in the same range as for alkanes. This will be important to understand the results for transition states based on forward and reverse reactions.

A closer look at column 6 reveals that the deviations can be grouped into several categories. For example, formation of primary alkyl radicals from *n*-alkanes is predicted by ab initio calculations to require about 0.7−1.15 kcal/mol more energy than estimated from group additivity theory. (Taking contribu-

TABLE 3: CBS-Q Calculated Bond Dissociation Energies and Entropies for C_1 to C_5 Alkanes and Their Comparison with GA Estimates

(a)

reaction	BDE ab initio @ 0 K [kcal/mol]	BDE ab initio @ 298 K [kcal/mol]	ΔBDE (thermal) [kcal/mol]	BDE GA [kcal/mol]	ΔBDE @ 298 K [kcal/mol]
H2 ⇒ H + H	104.43	106.32	0.89	104.2	1.12
		Primary H			
CH4 ⇒ CH3 + H	103.71	105.40	1.69	105.10	0.30
C2H6 ⇒ C2H5 + H	99.93	101.66	1.73	101.10	0.56
C3H8 ⇒ *n*-C3H7 + H	100.30	101.99	1.70	101.10	0.89
n-C4H10 ⇒ *n*-C4H9 + H	100.29	101.91	1.63	101.10	0.81
n-C5H12 ⇒ *n*-C5H11 (2) + H	100.60	102.25	1.65	101.10	1.15
i-C4H10 ⇒ *i*-C4H9 (1) + H	101.03	102.79	1.76	101.10	1.69
i-C5H1I2 ⇒ *i*-C5H11 (1)+H	100.62	102.13	1.61	100.70	1.43
i-C5H12 ⇒ *i*-C5H11 (4) + H	99.88	101.56	1.68	100.70	0.86
q-C5H12 ⇒ *q*-C5H11 + H	101.65	103.32	1.67	101.10	2.22
		Secondary H			
C3H8 ⇒ *i*-C3H7 + H	97.36	99.19	1.83	98.45	0.74
n-C4H10 ⇒ *n*-C4H9 (2) + H	97.77	99.51	1.74	98.45	1.06
n-C5H12 ⇒ *n*-C5H11 (2)+ H	97.66	99.33	1.68	98.45	0.88
n-C5H12 ⇒ *n*-C5H11 (3) + H	98.50	100.06	1.56	98.45	1.61
i-C5H12 ⇒ *i*-C5H11 (3) + H	97.68	99.40	1.72	97.65	1.75
		Tertiary H			
i-C4H10 ⇒ *tert*-Butyl + H	95.91	97.87	1.96	96.50	1.37
i−C5H12 ⇒ *i*-C5H11 (2) + H	96.29	98.31	2.02	95.70	2.61

(b)

reaction	ΔS^{298} ab initio [cal mol^{-1} K^{-1}]	ΔS^{298} GA [cal mol^{-1} K^{-1}]	$\Delta\Delta S^{298}$ [cal mol^{-1} K^{-1}]	radical classification HBI[27]	radical classification Cohen[26]
H2 ⇒ H +H	23.72	23.60	0.12	N/A	N/A
		Primary H			
CH4 ⇒ CH3 + H	29.35	29.30	0.04	N/A	N/A
C2H6 ⇒ C2H5 + H	32.06	32.19	−0.14	CCJ	I
C3H8 ⇒ *n*-C3H7 + H	32.18	32.19	−0.01	RCCJ	I
n-C4H10 ⇒ *n*-C4H9 + H	32.33	32.19	0.14	RCCJ	I
n-C5H12 ⇒ *n*-C5H11 + H	32.77	32.19	0.58	RCCJ	I
i-C4H10 ⇒ *i*-C4H9 (1) + H	33.39	33.30	0.09	isobutyl	I
i-C5H12 ⇒ *i*-C5H11 (1)+ H	30.96	31.12	−0.15	isobutyl	I
i-C5H12 ⇒ *i*-C5H11 (4) + H	30.78	30.82	−0.03	RCCJ	I
q-C5H12 ⇒ *q*-C5H11 + H	33.85	33.99	−0.14	neopentyl	I
		Secondary H			
C3H8 ⇒ *i*-C3H7 + H	31.58	31.91	−0.33	CCJC	IIb
n-C4H10 ⇒ *n*-C4H9 (2) + H	33.28	33.91	−0.63	RCCJC	IIb
n-C5H12 ⇒ *n*-C5H11 (2) + H	33.48	33.91	−0.43	RCCJC	IIb
n-C5H12 ⇒ *n*-C5H11 (3) + H	32.51	32.30	0.21	RCCJCC	IIc
i-C5H12 ⇒ *i*-C5H11 (3) + H	31.48	32.63	−1.05	?*	?
		Tertiary H			
i-C4H10 ⇒ *tert*-butyl + H	31.80	31.26	0.53	tertalkyl	IIIa
i-C5H12 ⇒ *i*-C5H11 (2) + H	31.53	31.26	0.27	tertalkyl	IIIc

tions of different conformers in *n*-C_5H_{12} and *n*-C_5H_{11} (1) into account this range reduces to 0.75−1.0 kcal/mol.) Formation of 3-methyl-but-1-yl (*i*-C_5H_{11}(4)) falls into the same class, but not formation of 2-methyl-prop-1-yl (*i*-C_4H_9 (1)) and 2-methyl-but-1-yl (*i*-C_5H_{11}(1)). From column 4, we learn that the change of thermal energy upon bond dissociation is nearly constant for all primary and secondary alkyls (average value 1.69 ±0.07 kcal/mol) and only slightly larger for tertiary alkyl radicals (∼2 kcal/mol). Therefore, the explanation for the systematic variations must lie in the E_o energies (0 K energies) of the reactants and products. Bozzelli et al.[26] and Cohen[25] realized that a classification of radicals simply into primary, secondary, and tertiary classes is not sufficient. Consequently, both authors suggest finer classifications, which are shown in the last two column of Table 3b. It can be observed easily that the primary radicals with BDE's around 0.8 kcal/mol belong to the CCJ or RCCJ class, while those with higher BDE's are assigned to other classes. Also, all three secondary radicals of II_b type (Cohen) have very similar deviations in the BDE comparison, and the different classifications of both tertiary radicals accordingly to Cohen is in agreement with their deviating BDE differences. Taking all observation together, an interpretation of the results in Table 3a is possible. The BDE's calculated via group additivity are based on hydrogen bond increments (HBI) which are constant (101.1, 98.45, and 96.5 kcal/mol) for primary, secondary, and tertiary alkyl radicals, respectively. Only gauche interactions are taken into account (0.8 kcal/mol in alkanes[30] but 0.4 kcal/mol for a −CH2* radical site in gauche position to a CH_3 group). Thus, the group additivity based $\Delta_f H^{298}$ for radicals does not reflect the more detailed classifications chosen to describe the entropies and heat capacities accurately. Our ab initio results, however, reflect such small changes and suggest that a finer differentiation of the heat of formations is required as well. The large experimental error of $\Delta_f H^{298}$ of radicals in connection with equally large uncertainties of CBS-Q calculations for radicals prohibits at this stage a recommendation for more accurate HBI's.

Before we turn to the entropy results, we would like to mention that, lacking a more appropriate HBI class, we calculated the GAV for 3-methyl-but-2-yl, *i*-C_5H_{11}(3) with the HBI values for "RCCJC" radicals. Further, we note that there is a large difference in the ΔBDE^{298K} values for *tert*-butyl and

TABLE 4: Group Additivity Values for Transition State Supergroups, {C/C$_i$/H$_{3-i}$/−H/H} (i = 1−3), Belonging to Hydrogen Abstraction Reactions from Alkanes by H Atoms[a]

reaction type	reaction	$\Delta_f H^{298}$	S^{298}	C_p^{300}	C_p^{400}	C_p^{500}	C_p^{600}	C_p^{800}	C_p^{1000}	C_p^{1500}	$\nu_{imaginary}$
primary R−H	C2H6 + H	50.81	35.21	9.37	11.78	13.81	15.48	17.98	19.70	22.25	2227
	C3H8 + H	50.94	34.94	9.49	11.90	13.91	15.56	18.02	19.72	22.25	2223
	n-C4H10 + H	50.71	34.78	9.36	11.83	13.88	15.55	18.02	19.72	22.25	2225
	i-C4H10 + H	50.77	35.27	9.37	11.73	13.70	15.32	17.79	19.53	22.14	2209
	n-C5H12 + H	50.70	34.71	9.47	11.92	13.95	15.60	18.05	19.74	22.25	2225
	i-C5H12 + H (1)	50.51	34.73	9.60	12.14	14.15	15.76	18.13	19.78	22.27	2210
	i-C5H12 + H (4)	50.43	34.38	9.65	12.10	14.13	15.77	18.19	19.85	22.31	2233
	q-C5H12 + H	50.88	34.82	9.48	11.97	13.97	15.59	17.99	19.66	22.20	2204
{C/C/H2/−H/H)	average	50.72	34.85	9.47	11.92	13.94	15.58	18.02	19.71	22.24	2219
forward rxn	mean dev.	0.17	0.29	0.11	0.14	0.15	0.15	0.12	0.09	0.05	10.27
	C2H5 + H2	51.48	35.49	8.80	11.25	13.34	15.08	17.76	19.63	22.34	
	C3H7 + H2	51.27	35.08	8.87	11.32	13.39	15.11	17.77	19.62	22.33	
	n-C4H9 (1) + H2	51.12	34.78	9.24	11.62	13.49	15.15	17.75	19.58	22.31	
	i-C4H9 (1) + H2	50.31	35.31	8.96	11.30	13.29	14.98	17.62	19.51	22.33	
	n-C5H11 (1) + H2	50.78	34.26	9.62	11.81	13.68	15.28	17.83	19.62	22.34	
	i-C5H11 (1) + H2	50.31	35.01	9.24	11.68	13.66	15.31	17.85	19.65	22.39	
	i-C5H11 (4) + H2	50.80	34.55	8.70	11.16	13.25	14.98	17.68	19.55	22.30	
	q-C5H11 + H2	49.88	35.09	9.11	11.52	13.45	15.05	17.56	19.39	22.14	
{C/C/H2/−H/H}	average	50.74	34.95	9.07	11.45	13.44	15.12	17.73	19.57	22.31	
reverse rxn	mean dev.	0.55	0.40	0.30	0.22	0.16	0.12	0.10	0.08	0.07	
secondary R−H	C3H8 + H	53.21	14.71	8.94	10.78	12.37	13.72	15.71	17.01	18.75	2206
	n-C4H10 + H	53.01	14.71	8.68	10.69	12.37	13.74	15.74	17.02	18.74	2194
	n-C5H12 + H (2)	52.57	14.41	8.91	10.99	12.64	13.98	15.89	17.12	18.79	2194
	n-C5H12 + H (3)	52.79	14.63	8.42	10.54	12.31	13.73	15.74	17.01	18.72	2183
	i-C5H12 + H	53.12	14.48	8.86	10.76	12.40	13.74	15.70	16.97	18.70	2190
{C/C2/H/−H/H}	average	52.94	14.59	8.76	10.75	12.42	13.78	15.75	17.03	18.74	2193
forward rxn	mean dev.	0.26	0.14	0.22	0.16	0.13	0.11	0.08	0.06	0.03	8.26
	i-C3H7 + H2	53.70	15.17	8.76	10.52	12.08	13.44	15.52	16.91	18.79	
	n-C4H9 (2) + H2	53.17	15.47	8.85	10.32	11.76	13.60	15.25	16.69	18.69	
	n-C5H11 (2) + H2	52.92	14.98	9.73	10.99	12.20	13.40	15.38	16.75	18.71	
	n-C5H11 (3) + H2	52.41	14.55	8.93	10.03	11.36	12.69	14.91	16.43	18.56	
	i-C5H11 (3) + H2	52.60	15.66	7.71	9.41	11.08	12.60	14.97	16.55	18.63	
{C/C2/H/−H/H}	average	52.96	15.17	8.79	10.25	11.69	13.15	15.21	16.67	18.68	
reverse rxn	mean dev.	0.51	0.43	0.72	0.58	0.48	0.46	0.26	0.19	0.09	
tertiary R−H	*i*-C4H10 + H	53.70	−6.60	8.32	9.89	11.14	12.13	13.56	14.38	15.47	2175
	i-C5H12 + H	53.51	−6.77	7.87	9.71	11.15	12.21	13.66	14.45	15.48	2164
{C/C3/−H/H}	average	53.60	−6.69	8.09	9.80	11.15	12.17	13.61	14.41	15.48	2169
forward rxn	mean dev.	0.13	0.12	0.32	0.13	0.00	0.06	0.07	0.05	0.01	7.85
	t-butyl + H2	53.56	−7.00	9.03	10.45	11.54	12.45	13.76	14.52	15.64	
	i-C5H11 (2) + H2	52.13	−6.91	8.57	10.23	11.43	12.42	13.79	14.56	15.69	
{C/C3/−H/H}	average	52.84	−6.95	8.80	10.34	11.48	12.44	13.77	14.54	15.66	
reverse rxn	mean dev.	1.01	0.07	0.32	0.16	0.07	0.02	0.03	0.03	0.04	

[a] Estimated uncertainty in ΔH is 1.5 kcal/mol and in S^{298}, and $C_p(T)$ values is 1 cal mol^{-1} K^{-1}. See text for the definition of supergroups.

2-methyl-but-2-yl. The thermochemistry of *tert*-butyl radical is a topic of intensive debate,[54] and it is not clear whether ab initio results or experimental data are in error. For 2-methyl-but-2-yl, the steric interaction of the additional methyl group on the radical center seems to have a noticeable impact on its energy, so the use of the same HBI class as for *tert*-butyl could be an oversimplification.

Only a few entropy values are established experimentally for radicals (Table 2), and these values are all taken from the early "structure and properties" compilation.[48b] The remarkably large deviations between the NIST data and GA predictions for C_3 and C_4 species indicate a significant uncertainty in these entropies. Our entropy results compare in all cases better with the GA predictions, although deviations are still large in some cases. This is encouraging because our goal to derive GAV for transition state structures depends primarily on a good agreement with group additivity for stable molecules and radicals.

Some radicals investigated in this study have more than one low-energy conformer. As in the case of stable molecules, we would have to consider contributions of all these conformers for a fair comparison with the bulk entropies. As mentioned earlier, it is not the primary goal of this work to reproduce thermodynamic data of bulk material, so we conclude that inclusion of other conformers will further improve the agreement with GA. The calculated entropies of the radicals *q*-pentyl and *tert*-butyl deviate from the GA values by more than 1 cal mol^{-1} K^{-1}. In the case of *q*-pentyl, the deviation of +1.6 cal mol^{-1} K^{-1} is similar to that found for *q*-pentane (∼1.2 cal mol^{-1} K^{-1}). It could be due to the anharmonicity effects caused by crowding around the central C atom, thereby making the harmonic oscillator assumption less appropriate. To a certain extent, this explanation could also hold for *tert*-butyl; however, the entropy of *tert*-butyl is much closer to the GA value. The *tert*-butyl radical is special in the sense that its planar conformation possesses very high symmetry (similar to CH_3), which could lead to coupling effects and less accurate frequencies.

Deviations between our results and GA increase for secondary and tertiary C−H dissociation (see Table 3 (part b). The ΔS^{298} value for *i*-C_5H_{12} → *i*-C_5H_{11}(3) + H especially is very large, −1.05 cal mol^{-1} K^{-1}. This underlines our suspicion that treating 3-methyl-but-2-yl as an RCCJC-type radical (for the HBI calculation) might be a poor assumption.

In summary, we can say that the deviations between ab initio data and GA predictions are a little larger for radicals than for stable molecules. Experimental data for radicals have larger errors; therefore, stable molecules and the HBI method[26] use a

TABLE 5: Group Additivity Values for Transition State Supergroups, {C/C$_i$/H$_{3-i}$/−H/CH3} (i = 1−3), Belonging to Hydrogen Abstraction Reactions from Alkanes by CH_3 Radicals[a]

reaction type	reaction	$\Delta_f H^{298}$	S^{298}	c_p^{300}	c_p^{400}	c_p^{500}	c_p^{600}	c_p^{800}	c_p^{1000}	c_p^{1500}	$\upsilon_{imaginary}$
primary R−H	C2H6 + CH3	37.79	48.93	14.37	17.83	20.83	23.40	27.51	30.60	35.52	2544
	C3H8 + CH3	37.62	47.13	14.35	17.83	20.84	23.41	27.52	30.60	35.52	2544
	n-C4H10 + CH3	37.34	47.44	14.19	17.72	20.77	23.38	27.51	30.60	35.52	2545
	i-C4H10 + CH3	37.53	46.99	14.50	18.00	20.99	23.52	27.57	30.62	35.51	2547
	n-C5H12 + CH3	37.20	46.96	14.60	18.18	21.21	23.75	27.78	30.78	35.60	2545
	i-C5H12 + CH3 (1)	37.25	46.58	14.66	18.12	21.05	23.54	27.56	30.60	35.50	2548
	i-C5H12 + CH3 (4)	36.46	47.00	14.59	17.98	20.93	23.46	27.53	30.60	35.50	2546
	q-C5H12 + CH3	37.20	46.30	14.41	18.01	21.04	23.60	27.65	30.69	35.55	2555
(C/C/H2/−H/C/H3)	average[b]	37.30	46.91	14.46	17.96	20.96	23.51	27.58	30.64	35.53	2547
forward	mean dev[b]	0.40	0.37	0.16	0.16	0.14	0.13	0.09	0.07	0.03	3.49
	C2H5 + CH4	37.82	49.13	13.97	17.44	20.49	23.12	27.37	30.55	35.50	
	C3H7 + CH4	37.32	47.19	13.90	17.38	20.45	23.09	27.34	30.52	35.50	
	n-C4H9(1) + CH4	37.12	47.35	14.24	17.54	20.51	23.10	27.32	30.48	35.47	
	i-C4H9(1) + CH4	36.43	46.96	14.26	17.70	20.71	23.30	27.47	30.62	35.60	
	n-C5H11(1) + CH4	36.64	46.43	14.92	18.20	21.07	23.56	27.63	30.69	35.59	
	i-C5H11(1) + CH4	36.42	46.78	14.48	17.79	20.69	23.22	27.35	30.49	35.51	
	i-C5H11(4) + CH4	36.20	47.09	13.82	17.17	20.18	22.79	27.09	30.33	35.39	
	q-C5H11 + CH4	35.57	46.49	14.20	17.69	20.65	23.19	27.30	30.44	35.39	
{C/C/H2/−H/C/H3)	average[c]	36.85	46.90	14.22	17.61	20.60	23.17	27.36	30.52	35.49	
reverse	mean dev[c]	0.59	0.35	0.36	0.31	0.26	0.22	0.15	0.11	0.08	
secondary R−H	C3H8 + CH3	40.40	27.32	14.02	16.96	19.52	21.75	25.33	27.97	32.05	2529
	n-C4H10 + CH3	39.95	27.14	13.76	16.88	19.53	21.80	25.38	28.00	32.05	2528
	n-C5H12 + CH3 (2)	39.31	27.06	13.99	17.23	19.86	22.07	25.55	28.11	32.10	2530
	n-C5H12 + CH3 (3)	39.47	27.61	12.86	16.24	19.14	21.56	25.28	27.95	32.02	2530
	i-C5H12 + CH3	39.73	26.02	14.23	17.26	19.84	22.03	25.48	28.04	32.04	2537
{C/C2/H/−H/C/H3)	average	39.77	27.28	13.77	16.91	19.58	21.84	25.40	28.01	32.05	2531
forward	mean dev.	0.43	0.24	0.54	0.41	0.29	0.21	0.11	0.07	0.03	3.41
	i-C3H7 + CH4	40.26	27.70	14.01	16.83	19.36	21.60	25.21	27.89	31.99	
	n-C4H9(2) + CH4	39.49	27.82	14.10	16.64	19.06	21.78	24.96	27.69	31.89	
	n-C5 H11(2) + CH4	39.02	27.55	14.98	17.35	19.56	21.62	25.12	27.77	31.92	
	n-C5H11(3) + CH4	38.46	27.45	13.55	15.87	18.32	20.64	24.52	27.39	31.76	
	i-C5H11 (3) + CH4	38.58	27.13	13.25	16.04	18.66	21.01	24.82	27.64	31.87	
{C/C2/H/−H/C/H3)	average	39.16	27.53	13.98	16.55	18.99	21.33	24.93	27.67	31.89	
reverse	mean dev.	0.74	0.26	0.66	0.60	0.50	0.48	0.27	0.19	0.08	
tertiary R−H	*t*-C4H10 + CH3	41.21	5.14	13.12	15.83	18.14	20.11	23.21	25.37	28.86	2508
	i-C5H12 + CH3	40.72	4.46	12.93	15.97	18.44	20.47	23.51	25.58	28.94	2509
{C/C3/−H/C/H3}	average	40.97	4.80	13.02	15.90	18.29	20.29	23.36	25.48	28.90	2508
forward	mean dev.	0.34	0.48	0.13	0.09	0.21	0.25	0.21	0.15	0.05	0.35
	t-Butyl + CH4	40.44	4.65	14.00	16.54	18.68	20.53	23.44	25.52	28.85	
	i-C5H11(2) + CH4	38.71	4.25	13.81	16.62	18.88	20.77	23.67	25.70	28.97	
{C/C3/−H/C/H3)	average	39.57	4.45	13.90	16.58	18.78	20.65	23.55	25.61	28.91	
reverse	mean dev.	1.23	0.29	0.13	0.06	0.14	0.17	0.16	0.13	0.08	

[a] Estimated uncertainty in ΔH is 1.5 kcal/mol and in S^{298}, and $C_p(T)$ values is 1 cal mol^{-1} K^{-1}. See text for the definition of supergroups. [b] Without C2H6 + CH3 reaction in S. [c] Without C2H5 + CH4 in S average and q-pentyl + CH4 in H average.

quite coarse differentiation of radicals, which cannot take the impact of all possible structural interactions on the thermodynamic properties into account. The theoretical calculations also have higher error bars than those for stable molecules because the treatment of open-shell species imposes a higher challenge on the theory. We conclude that the theoretical calculations are accurate to within 2 kcal for ΔH, 2 cal mol^{-1} K^{-1} for entropy, and about 1 cal mol^{-1} K^{-1} for C_p. Although there is still room for improvement, we conclude that the agreement is good enough to derive reliable transition state properties.

Transition State Geometry and Reaction Coordinate Frequency. The preceding results for stable molecules and radicals showed the reliability of the chosen methodology in predicting H, S, and C_p properties. We used the same type of calculation to characterize the transition states of the reactions mentioned in the Introduction. Instead of presenting the detailed results of all 41 transition states (The list of geometrical and molecular properties of the transition states are available as Supporting Information), we will only discuss general findings and use the results for the transition states directly to derive thermodynamic properties of the reaction center.

All transitions states studied in this work have well-defined, tight geometries. The length of the abstracting primary, secondary, or tertiary C−H bond in reactions of alkanes with H atoms varies, respectively, from 1.409 to 1.428, 1.389 to 1.403, and 1.369 to 1.381 Å. In the case of abstraction by methyl, the corresponding bond lengths are in the range of 1.316−1.333, 1.300−1.303, and 1.282−1.292 Å. The forming H−H bond lengths are of magnitude 0.889, 0.905, and 0.919 Å, respectively, in the case of primary, secondary, and tertiary abstractions. The forming CH_3−H bond length in primary, secondary, and tertiary abstractions is found to be, respectively, 1.353, 1.376, and 1.389 Å. The C−H−X bond angle (X = H, CH_3) remains nearly linear.

The expectation value of the S^2 operator, $\langle S^2 \rangle$, which is a measure of the extent of spin contamination in the optimized wave function, was found to be less than 0.78 in all transition states. The magnitude of the imaginary frequency depends on the type of reaction, and it ranges from 2164i to 2233i cm^{-1} for the abstraction by H and from 2501i to 2555i cm^{-1} for the abstraction by CH_3. The imaginary frequencies observed for H abstraction by other alkyl radicals are even higher (2554i− 2572i cm^{-1}), and for the H_2 + H reaction, we obtained ν = 2393i cm^{-1}. For the H abstraction reactions from alkanes, we observe a small effect of the substitution pattern on the magnitude of the imaginary frequency.

Transferability of Group Values. One necessary requirement for group additivity to be successful in describing

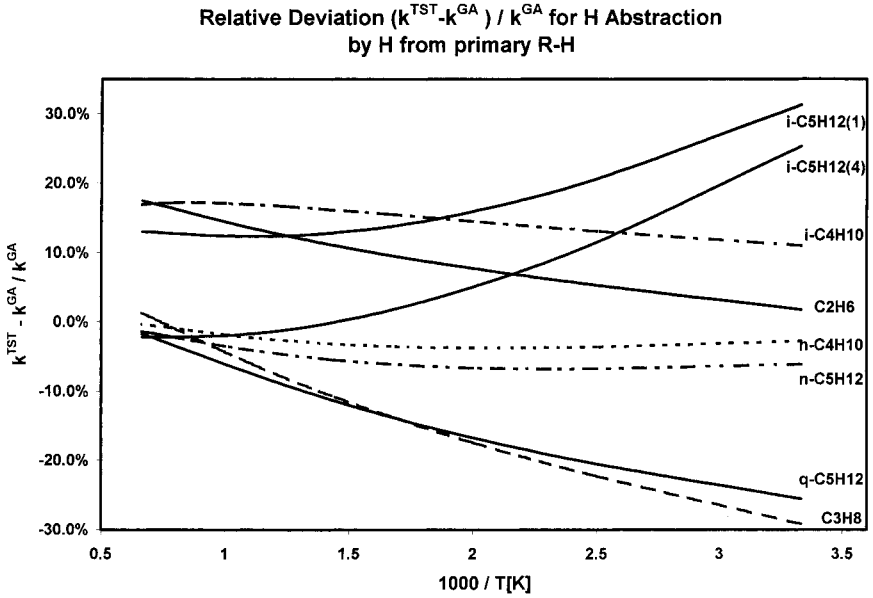

Figure 1. Comparison of individual TST rates with the rate predicted using group additivity for H abstraction from primary alkanes by hydrogen atoms. The small deviations show the accuracy of the group additivity approximation.

TABLE 6: Group Additivity Values for Transition State Supergroups of Symmetric {C/C$_i$/H$_{3-i}$/−H/C/C$_i$/H$_{3-i}$) (i = 0−3) and Mixed Symmetric Intermolecular Hydrogen Migration Reactions[a]

reaction type	reaction	$\Delta_f H^{298}$	S^{298}	C_p^{300}	C_p^{400}	C_p^{500}	C_p^{600}	C_p^{800}	C_p^{1000}	C_p^{1500}	$\upsilon_{imaginary}$
{H/−H/H}	H2 + H	60.35	39.13	7.62	8.49	9.26	9.91	10.88	11.51	12.31	2393
{C/H3/−H/C/H3}	CH4 + CH3	32.54	68.74	16.36	19.64	22.68	25.36	29.76	33.17	38.67	2545
{C/C/H2/−H/C/C/H2}	C2H6 + C2H5	43.49	27.26	12.17	15.72	18.69	21.18	25.13	27.98	32.36	2558
{C/C2/H/−H/C/C2/H}	C3H8 + *i*-C3H7	48.24	−14.52	12.09	14.44	16.39	18.12	20.84	22.72	25.38	2566
{C/C3/−H/C/C3}	*i*-C4H10 + *tert*-butyl	48.12	−61.47	11.97	13.88	15.13	16.10	17.42	18.07	19.21	2572
{C/H3/−H/H}	CH4 + H	45.98	54.25	11.30	13.56	15.66	17.45	20.24	22.29	25.41	
	H2 + CH3	46.61	54.33	11.13	13.43	15.52	17.33	20.17	22.27	25.52	2234
	average	46.30	54.29	11.22	13.50	15.59	17.39	20.21	22.28	25.47	
{C/C2/H/-H/C/C/H2}	C3H8 + C2H5	45.47	7.23	11.80	14.84	17.37	19.53	22.94	25.34	28.88	2554
	C2H6 + *i*-C3H7	45.29	7.42	12.19	15.10	17.55	19.66	22.97	25.32	28.84	
	average	45.38	7.33	12.00	14.97	17.46	19.59	22.95	25.33	28.86	
{C/C3/−H/C/C/H2)	*i*-C4H10 + C2H5	45.86	−17.45	11.00	13.81	16.07	17.95	20.85	22.77	25.70	2565
	C2H6 + *tert*-butyI	45.05	−18.13	12.28	14.91	16.94	18.65	21.22	22.96	25.71	
	average	45.46	−17.79	11.64	14.36	16.51	18.30	21.04	22.86	25.71	
{C/C3/−H/C/C2/H}	*i*-C4H10 + *i*-C3H7	47.68	−39.15	11.07	13.21	14.94	16.44	18.72	20.13	22.20	2572
	C3H8 + *t*-butyl	47.05	−40.01	11.95	14.04	15.64	17.01	19.06	20.35	22.26	
	average	47.36	−39.58	11.51	13.62	15.29	16.73	18.89	20.24	22.23	

[a] These supergroups are of use in estimating the hydrogen abstraction rates from alkanes by alkyl radicals.

thermodynamic properties of transition states is the constancy of the ΔH^{298}, S^{298}, and C_p^T supergroup values for a homologous series of reactions. To verify this, we have calculated the GAV for the supergroups of the transition states for all reaction types studied in this work. The results are given in Tables 4−6. The GAV for stable reactants were taken from ref 30, and those for all alkyl radicals were obtained with the HBI method of Bozzelli et al.[26] Table 4 contains the results for H abstraction reactions from alkanes by H atoms. Table 5 lists the results for abstraction by CH_3, and Table 6 contains the supergroup GAV of the remaining intermolecular H migration reactions given in the Introduction. Results are presented for both forward and reverse reactions, whenever available.

Table 4 clearly shows how well supergroup GAV's are defined for our first test set. It is divided into three main sections containing the results for primary, secondary, and tertiary H atoms abstractions. Each section separately contains the results for forward and reverse reactions to allow comparison of both data sets. The averaged H, S, and C_p supergroup GAV's for primary R−H sites (in forward and reverse direction) agree excellently, and the standard deviation especially for the forward reaction is small. The good agreement underlines in part our assumption that some of the errors will cancel out because we use only differences. However, a closer look at the BDE's in Table 3 suggests the great agreement seen between forward and reverse reactions to be fortuitous. The averaged difference found for the BDE's of primary R−H between ab initio and GA is very similar to the difference in dissociation energy for H_2, so both errors largely cancel each other out. Our discussion of Table 3 also explains why the standard deviation for the reverse reaction is much higher than that for the forward reaction.

Fluctuations of the supergroup GAVs for secondary and tertiary H abstraction by H atoms are also very small. Again, the reverse reaction shows for known reasons higher fluctuations than the forward reactions. The reaction *i*-C_5H_{11}(3) + H_2 especially worsens the agreement for the C_p^T data. As we pointed out earlier, we used RCCJCC HBI values to calculate the group additivity properties for this radical. The large deviations seen in Table 4 emphasize that this assignment leads to inaccurate results. We studied only two representative tertiary H abstraction reactions. With exception of the $\Delta_f H^{298}$ GAV for the reverse reactions, both data sets alone agree very well. However, the

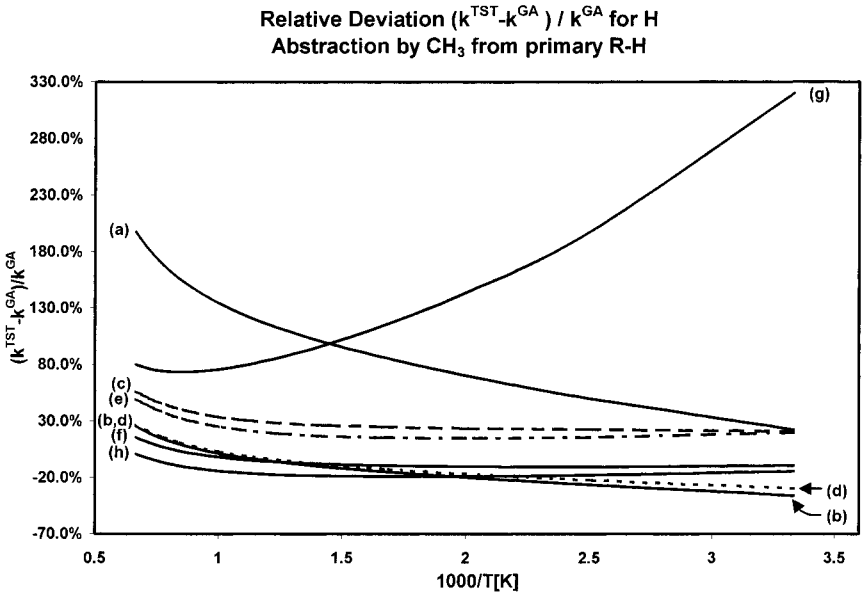

Figure 2. Comparison of individual TST rate calculations with the rate predicted using group additivity. H abstraction from primary alkanes by methyl radicals. Legend: (a) C_2H_6, (b) C_3H_8, (c) *n*-C_4H_{10}, (d) *i*-C_4H_{10}, (e) *n*-C_5H_{12}, (f) *i*-C_5H_{12} (1), (g) *i*-C_5H_{12} (4), and (h) *q*−C_5H_{12}.

averaged values for forward and reverse reactions differ noticeably. Future improvements in experiment and theory are necessary to close this gap.

In our evaluation of the thermochemical supergroup properties, we did not explicitly consider contributions of additional low-energy conformers because we assumed that the transition states will have similar contributions so that they cancel out. However, we verified that we used the lowest-energy conformation of the reactants and its corresponding transition state structure. The same holds for the reverse reaction starting from the product side. In the case of branched alkanes, we corrected GA-based heats of formation by 0.8 kcal/mol per additional gauche interaction[22] and those of branched alkyl radicals by 0.4 kcal/mol (this value was deduced from hindrance potential calculations).

Comparison of "Supergroup" Predicted Rate with TST Rates—A Test for Rate Prediction. One important question to ask at this point is how accurate the reaction rates based on supergroups will be as compared to individual TST calculations. Figure 1 addresses this question for the H abstraction from primary alkanes by H atoms. In this figure, we present the relative difference of rates for individual reactions, k^{TST}, compared to the GA-based rate prediction, k^{GA}. The rate without tunneling, k^{TST}, is calculated with transition state theory via

$$k^{TST}(T) = N_A k_B T/hQ^{\ddagger}/(Q_A Q_B) \exp(-E_o/(k_B T))$$

where N_A is Avogadro's number, E_0 is the ZPE-corrected barrier height, and the Q's are the molecular partition functions. All information needed is available from the calculation of the thermodynamic properties of the stable molecules, radicals, and transition states. In principle, k^{TST} could also be calculated via eq 1, but it is more convenient to use partition functions if available. All rates shown in Figure 1 are based on one C−H site and are therefore directly comparable. The plots consider only forward reactions. A deviation of +100% in the difference plot ($k^{TST} - k^{GA}/k^{GA}$) means that the TST rate is a factor of 2 larger than the GA rate. Similarly, a −50% deviation implies that k^{TST} is a factor of 2 slower than k^{GA}. Thus, Figure 1 shows that all TST rates are within a factor of 2 of the GA predicted rate. Most of the differences at low temperatures are due to small fluctuations in $\Delta H^{\ddagger}$; e.g., the relative deviation of $\sim$ +30% for *i*-C_5H_{12}(1) corresponds to a $\Delta\Delta G^{\ddagger}$ of $\sim$0.3 kcal/mol, which is well within the expected accuracy. Differences in the TST rates for secondary and tertiary R−H sites are also found to be within a factor of 2. It should be noted that the mismatch observed here between TST and GA rates (uncorrected for tunneling) reflects primarily the effect of averaging the thermochemical properties of "supergroup" on an individual reaction rate. This relative performance will not change with the inclusion of one-dimensional tunneling correction, since the latter depends primarily upon the shape (barrier height and the barrier width) of the reaction potential. As can be seen from Tables 4 and 5, the magnitude of the imaginary frequency remains nearly the same (within $\pm$15 cm^{-1}) so that contributions from tunneling will not vary significantly within a given type of reaction.

We now turn to the results for H abstraction by CH_3. From Table 5, we learn that the agreement between the individual supergroup GAV's is still good but not as good as that seen for the abstraction reactions by H atoms. Within the error bars, we see that the results for forward and reverse reactions overlap. There seem to be many reasons why the agreement is a little worse. First, we noted that the error in the calculated H_2 dissociation energy is fortunately of the same amount of discrepancies as those in the R−H dissociation. This is different for CH_3 because ab initio and GA BDE's for methane agree within 0.3 kcal/mol. This worsens the agreement between forward and reverse reactions. A second reason seems to be the stronger impact that an attacking CH_3 radical can have on the TS. In Table 5, we have seen that the heat of formation of the reaction of *i*-C_5H_{12}(4) + CH_3 does not match well into the set. In the reaction case of *n*-C_5H_{12} + CH_3 leading to the *n*-C_5H_{11}(3) radical, we found that the entropy and low-temperature C_p data differ from the remaining reactions. The TS could have a significantly different distribution of conformers than *n*-pentane so that our assumption that the conformer contributions will cancel in the GAV calculations could be poor in this case. In the case of C_2H_6 + CH_3, we find a larger entropy value than expected. A closer look on the hindrance barrier for CH_3 rotation reveals an explanation. The forming CH_3−H bond in the abstraction process reduces the hindrance barrier for the CH_3 rotation from about 3.0 kcal/mol in ethane to 2.35 kcal/mol in the transition state. This is a special feature of ethane

since the barriers remain roughly unchanged in, e.g., propane and *t*-butane. Because the reaction of CH_3 with ethane is a special case, we disregard it while averaging the entropy value of the {C/C/H2/−H/C/H3} group in both, forward and reverse directions.

Despite some deviations the overall consistency of the supergroup GAV is good and proves our concept. Thus, we proceed and compare the GA-based (generalized) reaction rate with individual transition state theory-based rates (Figure 2). For most of the reactions of primary C−H sites we find as for the reactions with H atoms agreement within better than a factor of 2. Only the earlier discussed special cases deviate more. Because of the lowered barrier in the reaction of 2-methylbutane with methyl radical to form 2-methylbut-1-yl radical, this reaction is at low temperatures nearly three times as fast as all other primary H abstractions by CH_3. With increasing temperatures, the rate approaches the GA rate. The $C_2H_6 + CH_3$ reaction behaves in the opposite manner. Caused by the increased reaction entropy, the abstraction rate becomes faster at higher temperatures. Both sets of GAV's derived from the forward reaction of H abstraction from secondary and tertiary C−H agree very well (not shown), so TST- and GA-based rates are very close.

Splitting Supergroups into "Benson" Groups. Having seen that GA-based rates can be useful for rate predictions, we now turn back to the supergroups. The supergroups characterized in the preceding paragraphs are very large and are not really in the spirit of group additivity. One reason is that they contain several polyvalent atoms and violate Benson's definition of a group. More of practical importance is the fact that permutations of individual atoms in such large supergroup will evidently lead to a large number of different supergroups, which makes characterization of them more elaborate and the whole methodology less useful. Therefore, we need to divide the supergroups into smaller fraction or groups in the sense of Benson. An obvious choice in our case is to take the polyvalent atoms as center of the new groups. For our six supergroups (SG) discussed so far, splitting could be done as follows:

$$SG^{I} = \{C/C/H2/-H/H\} = \{C/C/H2/-H\} + \{-H/C/H\} + \{H/-H\}$$

$$SG^{II} = \{C/C2/H/-H/H\} = \{C/C2/H/-H\} + \{-H/C/H\} + \{H/-H\}$$

$$SG^{III} = \{C/C3/-H/H\} = \{C/C3/-H\} + \{-H/C/H\} + \{H/-H\}$$

$$SG^{IV} = \{C/C/H2/-H/C/H3\} = \{C/C/H2/-H\} + \{-H/C2\} + \{C/H3/-H\}$$

$$SG^{V} = \{C/C2/H/-H/C/H3\} = \{C/C2/H/-H\} + \{-H/C2\} + \{C/H3/-H\}$$

$$SG^{VI} = \{C/C3/-H/C/H3\} = \{C/C3/-H\} + \{-H/C2\} + \{C/H3/-H\}$$

SG^{I}−SG^{III} describe the transition states for H abstraction by H, and the remaining three SG's correspond to CH_3 as abstracting species. Two out of three subgroups are constant in a set of SG's, and the third group is a common group in the respective abstraction reaction by H and CH_3. A quick test to see if such a splitting scheme could work is to compare the differences of SG pairs with each other. $SG^{I} - SG^{II}$ and $SG^{IV} - SG^{V}$ should both be equal to {C/C/H2/−H} − {C/C2/H/−H}. Similarly, the three differences $SG^{I} - SG^{IV}$, $SG^{II} - SG^{V}$, and $SG^{III} - SG^{VI}$ should all have the value {−H/C/H} + {H/−H} − {−H/C2} − {C/H3/−H}. Table 7 shows that such a splitting scheme could indeed work and that the group values are relatively constant. The C_p^T results especially support this conclusion. On the other hand, deviations in the differences for H^{298} and S^{298} are large enough to fear that further averaging to fit the SG data into this splitting scheme would undermine the accuracy.

The main argument against this idea is that the central groups {−H/C/H} and {−H/C2} are kept constant throughout and are treated as independent of the nature of the C atom(s). The properties of the C−H−H and C−H−C reaction centers will certainly depend on the nature of the C atoms bound to the migrating hydrogen. For example, if both C atoms in C−H−C are of the same nature as that in "symmetric" reactions between methane and methyl then both C−H distances will be equal. This is not the case for different C sites. Near the transition state, the geometrical parameters of the reaction center are very sensitive to the relative bond strength of the forming and breaking bonds. This suggests differentiating the carbons based on the substituents attached to it (e.g., C^m, C^p, C^s, and C^t). Such an extended interaction has already been considered in the characterization of alkyl radicals.[24−26] For example, Lay et al.[26] distinguish between four different primary alkyl radicals because the substitution pattern on the adjacent carbon atom has an impact on the $*CH_2-$ moiety.

Thus, we have strong arguments to differentiate with respect to the neighboring C sites as well. Doing so, we obtain four types of {−H/C^i/H} groups and 10 types of {−H/C^i/C^j} groups, with *i* and *j* denoting methyl, primary, secondary, or tertiary carbon sites. Together with the {C/C/H2/−H}, {C/C2/H/−H}, {C/C3/−H}, and {H/−H} groups, we end up with 18 groups and only six supergroups so far. To resolve this problem, we extended the reaction set by including five symmetric H migration reactions, viz., $H + H_2$, $CH_3 + CH_4$, $C_2H_5 + C_2H_6$, i-$C_3H_7 + C_3H_8$, and t-C_4H_9+i-C_4H_{10} as well as the corresponding "mixed" reactions ($H + CH_4$, $C_2H_5 + C_3H_6$ (primary/secondary pair), and $C_2H_5 + i$-C_4H_{10} (primary/tertiary pair) and i-$C_3H_7 + i$-C_4H_9 (secondary/tertiary pair). The results for the nine new supergroups are given in Table 6. This leads to a total of 15 supergroups and 20 groups, since two new groups ({−H/H2} and {C/C/H3/−H}) have to be introduced. With the idea in mind that the central {−H/X/Y} group should be a measure of the asymmetry in the forming and breaking bonds of a transition state, we define all five {−H/X2} groups to be zero. Determination of the group values of the remaining 15 groups then becomes straightforward, and the results are presented in Table 8.

Before proceeding further with the group values, it is appropriate to have a closer look at Table 6. The nine supergroups presented therein are essentially derived from a single reaction of each category. In the case of (−H/H) and (C/H3/−H), the reason is obvious as one is left with a unique choice. However, this is not true for the remaining supergroups. For example, the supergroup (C/C/H2/−H/C/C/H2) could have been derived from any other reaction in the homologous series of primary hydrogen abstraction by a primary alkyl radical as well. On the basis of the constancy of the six supergroup values shown in Tables 4 and 5, we restrict ourselves to the first member for the sake of computational efficiency.

Most of the thermodynamic properties obtained for the new "transition state-specific" groups seem reasonable. The contribu-

TABLE 7: Analyzing Supergroups: Indication of Constant Supergroup Differences between H and CH_3 Abstractions

SG*−SG**	$\Delta_f H^{298}$	S^{298}	C_p^{300}	C_p^{400}	C_p^{500}	C_p^{600}	C_p^{800}	C_p^{1000}	C_p^{1500}
{C/C/H2/−H} − {C/C2/H/−H}									
$SG^{I}-SG^{II}$	−2.22	20.02	0.49	1.19	1.63	1.88	2.39	2.79	3.57
$SG^{I}-SG^{V}$	−2.38	19.49	0.47	1.06	1.49	1.75	2.30	2.73	3.54
difference	0.16	0.54	0.03	0.13	0.14	0.13	0.09	0.06	0.03
{C/C/H2/−H} − {C/C3/−H}									
$SG^{I}-SG^{III}$	−2.49	41.72.	0.82	1.61	2.38	3.04	4.18	5.16	6.71
$SG^{IV}-SG^{VI}$	−3.18	42.28	0.88	1.55	2.24	2.87	4.01	5.03	6.61
difference	0.69	−0.56	−0.06	0.07	0.14	0.18	0.17	0.13	0.10
{C/C2/H/−H} − {C/C3/−H}									
$SG^{II}-SG^{III}$	−0.27	21.70	0.33	0.43	0.74	1.16	1.79	2.37	3.14
$SG^{V}-SG^{VI}$	−0.80	22.79	0.41	0.49	0.75	1.12	1.71	2.30	3.06
difference	0.53	−1.10	−0.08	−0.06	−0.01	0.05	0.08	0.07	0.07
{−H/C/H} + {H/−H} − {H/C2} − {C/H3/−H}									
$SG^{I}-SG^{Iv}$	13.64	−12.01	−5.07	−6.10	−7.08	−7.99	−9.59	−10.94	−13.23
$SG^{II}-SG^{V}$	13.49	−12.54	−5.10	−6.23	−7.23	-8.12	−9.68	−11.00	−13.26
$SG^{III}-SG^{VI}$	12.95	−11.44	−5.02	−6.17	−7.22	−8.17	−9.76	−11.07	−13.34
average	13.36	−12.00	−5.06	−6.17	−7.18	−8.09	−9.68	−11.00	−13.28
st dev	0.36	0.55	0.04	0.06	0.08	0.09	0.08	0.06	0.05

TABLE 8: "Transition-State Specific" Group Additivity Values (GAV) for Hydrogen Abstraction Reactions

group name	$\Delta_f H^{298}$	S^{298}	C_p^{300}	C_p^{400}	C_p^{500}	C_p^{600}	C_p^{800}	C_p^{1000}	C_p^{1500}
{−H/X_2}, with X = H, C^m, C^p, C^s, C^t	0.00	0.00	0.00	0.00	0.00	0.00	0.00	0.00	0.00
{−H/H}	30.17	19.56	3.81	4.25	4.63	4.96	5.44	5.75	6.16
{−H/C^m/H}	−0.15	0.36	−0.77	−0.57	−0.38	−0.25	−0.11	−0.06	−0.02
{−H/C^p/H}	−1.18	1.71	−0.62	−0.42	−0.29	−0.20	−0.13	−0.10	−0.06
{−H/C^s/H}	−1.34	2.58	−1.08	−0.96	−0.77	−0.55	−0.38	−0.27	−0.14
{−H/C^t/H}	−0.87	4.30	−1.30	−1.05	−0.82	−0.66	−0.43	−0.31	−0.21
{−H/C^m/C^p}	−0.92	−1.09	0.08	0.10	0.09	0.07	0.02	0.00	0.00
{−H/C^m/C^s}	−0.62	−0.08	−0.46	−0.13	0.04	0.10	0.10	0.07	0.03
{−H/C^m/C^t}	0.64	0.68	−0.73	−0.49	−0.34	−0.25	−0.15	−0.12	−0.06
{−H/C^p/C^s}	−0.48	0.96	−0.13	−0.11	−0.08	−0.06	−0.03	−0.02	−0.01
{−H/C^p/C^t}	−0.34	−0.68	−0.43	−0.44	−0.40	−0.34	0.24	−0.16	−0.07
{−H/C^s/C^t}	−0.82	−1.59	−0.52	−0.54	−0.47	−0.38	−0.24	−0.15	−0.06
{C/H3/−H)	16.27	34.37	8.18	9.82	11.34	12.68	14.88	16.59	19.33
{C/C/H2/−H}	21.74	13.63	6.08	7.86	9.34	10.59	12.56	13.99	16.18
{C/C2/H/−H}	24.12	−7.26	6.05	7.22	8.19	9.06	10.42	11.36	12.69
{C/C3/−H}	24.06	−30.73	5.99	6.94	7.56	8.05	8.71	9.04	9.80

tions of the central groups, {−H/X/Y}, in the reaction center to ΔH^{298}, S[29,8] and C_p^T are small. This is in agreement with our picture that these groups present a measure of the asymmetry from those of symmetric transition states. Most of the thermodynamic information is consequently absorbed in the {$C/C_i/H_{3-i}$/−H} and {−H/H} groups. C_p^T contributions of these groups change in a monotonic way. Changes in S and C_p contributions follow in general a trend when going from methyl to tertiary carbon; however, this is not true for ΔH. The heat of formation contribution continues to decrease from C^m to C^s. However, it increases for a tertiary C site (C^t) in both the (−H/C^i/H) and {$C/C_i/H_{3-i}$/−H} groups. This observation should not be over emphasized because of the uncertainties in ab initio and experimental heats of formation for *t*-butane and *tert*-butyl systems.

Reaction Rate Estimation Based on Group Additivity—Comparison with Experimental Rates. We now use the newly developed GAV to estimate reaction rates. Rates for small alkanes are compared with kinetic data from the NIST database,[55] with predictions based on the work of Ranzi et al.,[21] and with rate constants used in the modeling of heptane oxidation by Curran et al.[56] Contributions due to tunneling are approximated with the Wigner formalism.[46] The imaginary frequencies are listed in Tables 5−7, and we use the averaged imaginary frequencies of a series. The heat capacity data are fitted to a fourth-order polynomial to simplify their use. Instead of comparing predicted rates to individual reaction rates given in the NIST database, we have chosen to compare our predictions with a generalized rate extracted from several individual reactions of the database. We fitted individual reactions with Arrhenius or modified Arrhenius expressions and subsequently averaged them by determining a new (modified) Arrhenius expression as a representative of them. In a similar manner, we used Ranzi et al.'s kinetic data. Rate comparison is restricted to temperatures between 300 and 1500 K, the range for which group additivity C_p data are available. Figure 3 shows the results for the primary and secondary R−H + H reaction. The rates are given per hydrogen. In most cases, our GA-based reaction rates are a little higher than the references, especially for H abstraction from secondary C−H sites. In both cases, the differences are largest with respect to the rates of Ranzi, followed by those of Curran. The agreement with NIST data is excellent for primary H abstraction. For the reaction of secondary C−H with hydrogen atoms, our prediction is at high temperatures higher than those of our fit from the NIST database by about a factor of 2, and this factor increases at low temperatures. In view of the very few experimental data available for secondary C−H abstractions, this deviation should be considered reasonable.

A comparison of predicted rates for H abstraction by CH_3 radicals is shown in Figure 4. Again, only reactions with primary and secondary alkanes are plotted. To calculate rates on the per C−H site basis, we had to incorporate the correct reaction path degeneracy factor. Using the symmetry factor of 6 for

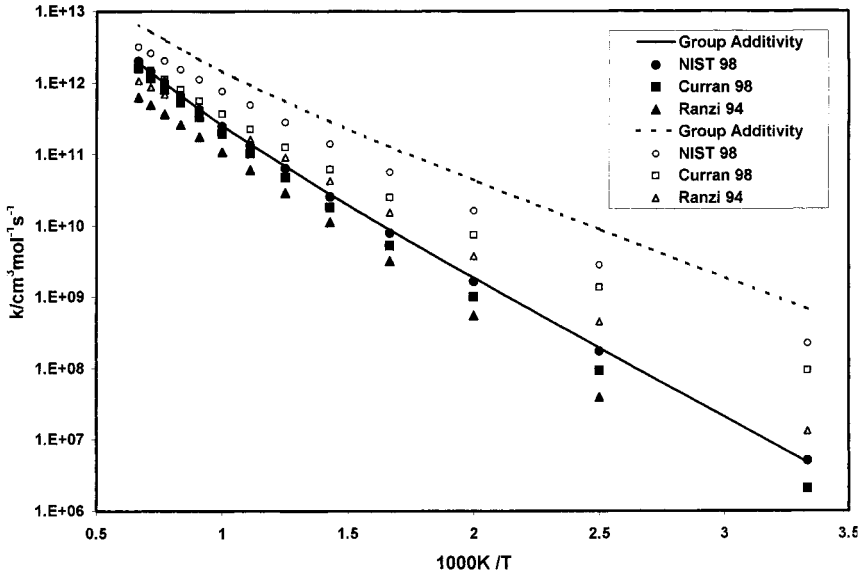

Figure 3. Comparison of group additivity predicted rates with literature. H abstraction from primary (solid symbols) and secondary (open symbols) alkanes by hydrogen atoms. References: NIST 98 data are based on ref 55, Curran 98 on ref 56, and Ranzi 94 on ref 21. The group additivity predictions are within a factor of 2 of the experimentally derived NIST values.

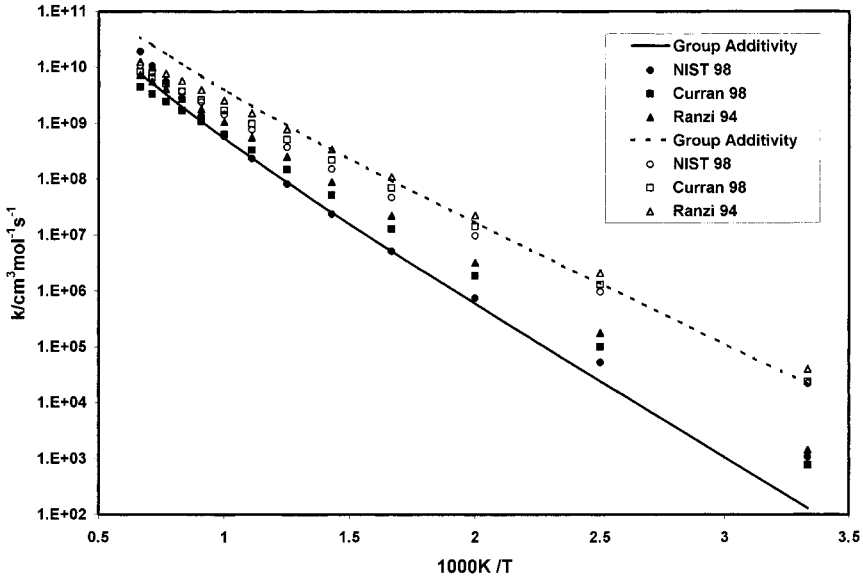

Figure 4. Comparison of with group additivity predicted rates with literature. H abstraction from primary (solid symbols) and secondary (open symbols) alkanes by methyl radicals. References: NIST 98 data are based on ref 55, Curran 98 on ref 56, and Ranzi 94 on ref 21. Note that the discrepancies between the predictions and the experimentally derived values are relatively small in the middle temperature range where the experimental data are most firmly established.

methyl, 18 for an alkane, and, e.g., 9 for abstractions from *n*-alkanes, we find that the ratio $\sigma(CH_3)\sigma(\text{alkane})/\sigma(\text{ts}) = 12$, although only six H atoms are involved. As the total rate is correct, we have to divide it by 6 to get the rate per hydrogen instead of dividing through the reciprocal of the symmetry ratio. The comparison shows good agreement at high temperatures in the case of primary H abstraction and better agreement at lower temperatures for secondary H abstraction.

It should be noted that Wigner's tunneling correction is a simplified approach and is known to underestimate the tunneling contributions. This might explain the discrepancy at low temperatures for methyl abstracting a primary H in Figure 4. However, the low-temperature discrepancies in Figure 3 have the opposite sign: the calculations using Wigner tunneling estimates are higher than the literature rate estimates. An improved treatment involving the intrinsic reaction coordinate potential energy surface such as multidimensional zero-curvature[57] and centrifugal dominant small-curvature methods[58] would be expected to reduce the uncertainties in our predictions. However, the uncertainties in the TST calculation (ignoring tunneling) due to uncertainties in the barrier height and activation entropy are likely to be at least as large as the errors introduced by our simple tunneling treatment. A rough estimate of the uncertainty in the supergroup values can be obtained by adding the error due to the group-additivity approximation (e.g., the range of the deviations between the group-additivity and individual-molecule calculations of ΔH, S^{298}, and $C_p(T)$) to the uncertainty in the thermochemical values of the reactants. CBS-Q is reported to give heats of formation accurate to about 1 kcal/mol,[43] and our comparisons between calculated and experimental entropies and heat capacities suggest they have uncertainties of about 0.5 cal mol^{-1} K^{-1}. Hence, we expect the supergroup ΔH values to be good to about 1.5 kcal/mol and the S^{298} and C_p values to be accurate to about 1 cal mol^{-1} K^{-1}. The experimental rate data are consistent with the group additivity rate estimates within these uncertainty bounds; in fact,

the agreement is slightly better than our uncertainty estimate would suggest, perhaps due to a favorable cancellation of errors.

Summary

We introduced the idea of characterizing thermodynamic properties of transition states in terms of Bensons group additivity method. The CBS-Q level of theory was used for energy calculations, and additional partial HF/6-31G(d′) optimizations were performed to obtain hindrance potentials for internal rotations. Coupling between internal and external rotation was taken into account as described by Pitzer et al. Comparison of our results of $\Delta_f H^{298}$, S^{298}, and $C_p(T)$ data for alkanes and alkyl radicals show good agreement with experimental data and GA predictions.

Applying the same methodology to the transition states for H abstraction from alkanes by H and CH_3 led to constant thermodynamic values for the reaction specific moiety in the transition state. The GAV of these so-called supergroups are further subdivided into smaller Benson-like groups, which allows a full description of these transition states via group additivity. Reaction rates calculated with the new GAV agree reasonably well with published kinetic information.

Using the concept of group additivity to predict reaction rates has several advantages over other known methods: (1) In general, GA can be used for all types of reactions and is not restricted to special cases. (2) The temperature behavior of rate constants is thermodynamically consistent and is not bound to Arrhenius forms. (3) Implementation in automated mechanism generating algorithms should be easy, since such packages have already codes to estimate thermodynamic data for stable species using GA. (4) Addition of non-nearest-neighbor interactions to the GAV allows differentiation of reactivity due to substitution effects. (5) The derivation of GAV for transition states from forward and reverse reactions allows a consistency check of the thermodynamic data of the reactants and products.

The observed good performance of our calculations on the well understood intermolecular H abstraction from alkanes by H and CH_3 encourages us to continue our efforts and to expand the studies to less well-known reaction types such as intramolecular abstraction (migration) reactions. We further plan to address the role of substituents on adjacent C sites in abstraction reactions.

Acknowledgment. This work was partially supported by National Computational Science Alliance under Grants CHE000004N and CHE000021N and utilized the Exemplar X-Class High-Performance Computing and UniTree Mass Storage Systems. We are grateful for financial support from the EPA Center for Airborne Organics, the NSF CAREER program, Alstom Power, Dow Chemical, and the Division of Chemical Sciences, Office of Basic Energy Sciences, Office of Energy Research, U.S. Department of Energy through Grant DE-FG02-98ER14914.

Supporting Information Available: MP2/6-31G(d′) optimized geometries, unscaled harmonic frequencies (in cm^{-1}), and rotational constants (in GHz) of the transition structures. This material is available free of charge via the Internet at http://pubs.acs.org.

Note Added after ASAP Posting. This article was posted ASAP without a description of the Supporting Information on 6/22/01. The correct version was posted on 6/25/01.

References and Notes

(1) Chinnick, S. J.; Baulch, D. L.; Ayscough, P. B. *Chemom. Intell. Lab. Syst.* **1988**, *5*, 39.
(2) Haux, L.; Cunin, P.-Y.; Griffiths, M.; Come, G.-M. *J. Chim. Phys.* **1988**, *85*, 739.
(3) Chevalier, C.; Warnatz, J.; Melenk, H. *Ber. Bunsen-Ges. Phys. Chem.* **1990**, *94*, 1362.
(4) Dente, M.; Pierucci, S.; Ranzi, E.; Bussant, G. *Chem. Eng. Sci.* **1992**, *47*, 2629.
(5) Chevalier, C.; Pitz, W. J.; Warnatz, J.; Westbrook, C. K.; Melenk, H. *Proc. Combust. Inst.* **1992**, *24*, 93.
(6) Blurock, E. S. *J. Chem. Inf. Comput. Sci.* **1995**, *35*, 607.
(7) Nehse, M.; Warnatz, J.; Chevalier, C. *Symp. (Int.) Combust., [Proc.]* **1996**, *26*, 773.
(8) Ranzi, E.; Faravelli, T.; Gaffuri, P.; Sogaro, A. *Combust. Flame* **1995**, *102*, 179.
(9) Ranzi, E.; Sogaro, A.; Gaffuri, P.; Pennati, G.; Westbrook, C. K.; Pitz, W. *Combust. Flame* **1994**, *99*, 201.
(10) Susnow, R. G.; Dean, A. M.; Green, W. H.; Peczak, P. *J. Phys. Chem. A* **1997**, *101*, 3731.
(11) Broadbelt, L. J.; Start, S. M.; Klein, M. T. *Comput. Chem. Eng.* **1996**, *20*, 113.
(12) Broadbelt, L. J.; Stark, S. M.; Klein, M. T. *Ind. Eng. Chem. Res.* **1995**, *34*, 2566.
(13) Broadbelt, L. J.; Stark, S. M.; Klein, M. T. *Ind. Eng. Chem. Res.* **1994**, *33*, 790.
(14) Green, W. H. Jr.; Moore, C. B.; Polik, W. F. *Annu. Rev. Phys. Chem.* **1992**, *43*, 591.
(15) Miller, W. H. *J. Phys. Chem. A* **1998**, *102*, 793.
(16) Chang, A. Y.; Bozzelli, J. W.; Dean, A. M. *Z. Phys. Chem.* **2000**, *214*, 1533.
(17) Barker, J. R. *Multiwell Software*, version 1.01; University of Michigan: Ann Arbor, MI, 1999.
(18) Blowers, P.; Masel, R. I. *AIChE J.* **1999**, *45*, 1794.
(19) Boock, L. T.; Klein, M. T. *Ind. Eng. Chem. Res.* **1993**, *32*, 2464.
(20) Denisov, E. In *General Aspects of the Chemistry of Radicals*; Alfassi,, Z. B., Ed.; Wiley: New York, 1999; Chapter 4, p 79 and references therein.
(21) Ranzi, E.; Dente, M.; Faravelli, T.; Pennati, G. *Combust. Sci. Technol.* **1994**, *95*, 1.
(22) Benson, S. W. *Thermochemical Kinetics*, 2nd ed.; Wiley-Interscience: New York, 1976.
(23) Yamada, T.; Lay, T. H.; Bozzelli, J. W. *J. Phys. Chem. A* **1998**, *102*, 7286.
(24) O'Neal, H. E.; Benson, S. W. *Int. J. Chem. Kinet.* **1969**, *1*, 221. O'Neal, H. E.; Benson, S. W. Thermochemistry of Free Radicals. In *Free Radicals*; Koshi, J. H., Ed.; Wiley: New York, 1973; pp 275−379.
(25) Cohen, N. *J. Phys. Chem.* **1992**, *96*, 9052.
(26) Lay, T. H.; Bozzelli, J. W.; Dean, A. M.; Ritter, E. R. *J. Phys. Chem.* **1995**, *99*, 14514.
(27) Bader, R. F. W.; Bayles, D. *J. Phys. Chem. A* **2000**, *104*, 5579.
(28) Cohen, N. *Int. J. Chem. Kinet.* **1982**, *14*, 1339; **1983**, *15*, 503; **1991**, *23*, 397 and 683.
(29) Truong, T. N. *J. Chem. Phys.* **2000**, *113*, 4957.
(30) Cohen, N.; Benson, S. W. The Thermochemistry of Alkanes and Cycloalkanes. In *The Chemistry of Alkanes and Cycloalkanes*; Patai, S., Rappoport, Z., Eds.; Wiley: New York, 1992.
(31) Pitzer, K. S.; Gwinn, W. D. *J. Chem. Phys.* **1942**, *10*, 428.
(32) Pitzer, K. S. *J. Chem. Phys.* **1946**, *14*, 239.
(33) Kilpatrick, J. E.; Pitzer, K. S. *J. Chem. Phys.* **1949**, *17*, 1064.
(34) Mazyar, O.; Green, W. H., Jr. Manuscript in preparation.
(35) McClurg, R. B.; Flagan, R. C.; Goddard, W. A. *J. Chem. Phys.* **1997**, *106*, 6675.
(36) Chuang, Y.-Y.; Truhlar, D. G. *J. Chem. Phys.* **2000**, *112*, 1221.
(37) Ayala, P. Y.; Schlegel, H. B. *J. Chem. Phys.* **1998**, *108*, 2314.
(38) East, A. L. L.; Radom, L. *J. Chem. Phys.* **1997**, *106*, 6655.
(39) Herschbach, D. R.; Johnston, H. S.; Pitzer, K. S.; Powell, R. E. *J. Chem. Phys.* **1956**, *25*, 736.
(40) Montgomery, J. A., Jr.; Ochterski, J. W.; Petersson, G. A. *J. Chem. Phys.* **1994**, *101*, 5900. Ochterski, J. W.; Petersson, G. A.; Montgomery, J. A., Jr. *J. Chem. Phys.* **1996**, *104*, 2598.
(41) Frisch, M. J.; Trucks, G. W.; Schlegel, H. B.; Scuseria, G. E.; Robb, M. A.; Cheeseman, J. R.; Zakrzewski, V. G.; Montgomery, J. A.; Stratmann, R. E.; Burant, J. C.; Dapprich, S.; Millam, J. M.; Daniels, A. D.; Kudin, K. N.; Strain, M. C.; Farkas, O.; Tomasi, J.; Barone, V.; Cossi, M.; Cammi, R.; Mennucci, B.; Pomelli, C.; Adamo, C.; Clifford, S.; Ochterski, J.; Petersson, G. A.; Ayala, P. Y.; Cui, Q.; Morokuma, K.; Malick, D. K.; Rabuck, A. D.; Raghavachari, K.; Foresman, J. B.; Cioslowski, J.; Ortiz, J. V.; Baboul, A. G.; Stefanov, B. B.; Liu, G.; Liashenko, A.; Piskorz, P.; Komaromi, I.; Gomperts, R.; Martin, A. L.; Fox, D. J.; Keith, T.; Al-Laham, M. A.; Peng, C. Y.; Nanayakkara, A.; Challacombe, M.; Gill, P. M. W.; Johnson, B.; Chen, W.; Wong, M. W.; Andres, J. L.; Gonzalez, C.; Head-Gordon, M.; Replogle, E. S.; Pople, J. A. *Gaussian 98*, Revision A.9; Gaussian, Inc.: Pittsburgh, PA, 1998.
(42) Scott, A. P.; Radom, L. *J. Phys. Chem. A* **1996**, *102*, 16502.

(43) Petersson, G. A.; Malick, D. K.; Wilson, W. G.; Ochterski, J. W.; Montgomery, J. A., Jr.; Frisch, M. J. *J. Chem. Phys.* **1998**, *109*, 10570.
(44) Curtiss, L. A.; Raghavachari, K.; Redfern, P. C.; Pople, J. A. *J. Chem. Phys.* **1997**, *106*, 1063.
(45) Chase, M. W., Jr.; Davies, C. A.; Downey, J. R., Jr.; Frurip, D. J.; McDonald, R. A.; Syverud, A. N. *J. Phys. Chem. Ref. Data* **1985**, *14 Suppl. No. 1*.
(46) Ritter, E. R.; Bozzelli, J. W. *Int. J. Chem. Kinet*. **1991**, *23*, 767.
(47) Hirschfelder, J. O.; Wigner, E. *J. Chem. Phys.* **1939**, *7*, 616.
(48) (a) *NIST Webbook* (http://webbook.nist.gov, accessed Sept 2000). (b) *NIST Standard Reference Database 25, Structure and Properties*, Version 2.02; National Institute of Science and Technology: Gaithersburg, MD, 1994.
(49) Chen, S. S.; Wilhoit, R. C.; Zwolinski, B. J. *J. Phys. Chem. Ref. Data* **1975**, *4*, 859.
(50) Gang, J.; Pilling, M. J.; Robertson, S. H. *J. Chem. Soc., Faraday Trans.* **1996**, *96*, 3509.
(51) DeTar, D. F. *J. Phys. Chem. A* **1998**, *102*, 5128.
(52) Yamada, C.; Hirota, E.; Kawaguchi, K. *J. Chem. Phys.* **1981**, *75*, 5256.
(53) Wormhoudt, J.; McCurdy, K. E. *Chem. Phys. Lett.* **1989**, *156*, 47.
(54) Smith, B. J.; Radom, L. *J. Phys. Chem. A* **1998**, *102*, 10787.
(55) *NIST Chemical Kinetics Database*, version 2Q98, Standard Reference Data Program, NIST, MD-20899; National Institute of Science and Technology: Gaithersburg, MD.
(56) Curran, H. J.; Gaffuri, P.; Pitz, W. J.; Westbrook, C. K. *Combust. Flame* **1998**, *114*, 149.
(57) Truhlar, D. G.; Garrett, B. C. *Annu. Rev. Phys. Chem.* **1984**, *35*, 159.
(58) Lu D. H.; Truong, T. N.; Melissas, V. S.; Lynch, G. C.; Liu, V. P.; Garrett, B. C.; Steckler, R.; Isaacson, A. D.; Rai, S. N.; Hancock, G. C.; Lauderdale, J. G.; Joseph, T.; Truhlar, D. G. *Comput. Phys. Commun.* **1992**, *71*, 235.